

# Selection and Estimation for Mixed Graphical Models

Shizhe Chen, Daniela Witten, and Ali Shojaie  
 Department of Biostatistics, University of Washington  
 szchen@uw.edu

October 31, 2013

## Abstract

We consider the problem of estimating a pairwise graphical model in which the nodes are of different types. In particular, we assume that each node, conditioned on all other nodes, has a distribution that is in the exponential family. To begin, we identify restrictions on the parameter space required for the existence of a well-defined joint density in this setting. Next we establish the consistency of the neighbourhood selection approach for graph reconstruction in high dimensions when the true underlying graph is sparse. Motivated by our theoretical results, we investigate the selection of edges between nodes of two different types, and show that efficiency can be gained if edge estimates obtained from the regressions of particular node types are used to reconstruct the graph. These results are illustrated with examples of Gaussian, binary, Poisson and exponential distributions. Our theoretical findings are corroborated by evidence from simulation studies. We apply the proposed method and competing approaches to a yeast eQTL data set consisting of gene expression and DNA sequence data.

**Keywords:** compatibility; conditional likelihood; exponential family; high-dimensional; model selection consistency; neighbourhood selection; pairwise Markov random field.

## 1 Introduction

An undirected graphical model, also known as a Markov random field, is a probabilistic model induced by a graph  $G$ . Specifically, suppose that we have  $p$  random variables represented as nodes of the graph  $G = (V, E)$  with the vertex set  $V = \{1, \dots, p\}$  and the edge set  $E \subseteq \{V \times V\}$ . In such models, an edge represents a conditional dependence relationship between the pair of random variables that it connects. Some early work addressed the issue of how to make valid statistical inference on data with a known graphical structure (see e.g. Besag 1974). The reverse problem of how to reconstruct the underlying graph from a set of  $n$  observations has attracted a lot of interest in recent years. This problem is particularly challenging in the high-dimensional setting, where  $p > n$  and  $p(p-1)/2$  edges must be estimated from  $n$  observations. An  $\ell_0$ -penalty approach to this problem, in which we seek to identify a subset of edges that provide the best fit to the data given the size of  $E$ , is computationally intractable. A popular alternative is to use an  $\ell_1$ -penalty, which yields a parsimonious edge set through a convex optimization problem; this problem is potentially tractable even when  $p$  is large.

In the high-dimensional setting, Gaussian graphical models have been studied extensively (see e.g. Meinshausen and Bühlmann 2006, Yuan and Lin 2007, Friedman et al. 2008, Rothman et al. 2008, Wainwright and Jordan 2008, Peng et al. 2009, Ravikumar et al. 2011). However, the inherent assumption of multivariate normality limits the flexibility of the Gaussian graphical model. Some attempts have been made to generalize the Gaussian graphical model to account for non-normality and outliers (among others, Miyamura and Kano 2006, Liu et al. 2009, Finegold and Drton 2011, Sun and Li 2012, Xue and Zou 2012, Voorman et al. 2013). However, these models cannot be easily generalized to certain types of data, for instance, to discrete variables.

A few authors have studied high-dimensional graphical models for other distributions. Graphical models for binary data have been studied by Lee et al. (2006), Höfling and Tibshirani (2009), and Ravikumar et al. (2010). Other high-dimensional parametric graphical models consisting of a single type of nodal variable include the multinomial (Jalali et al. 2011, Dai et al. 2012), Poisson (Allen and Liu, 2012), and any univariate distribution within the exponential family (Yang et al., 2012).

In this paper, we consider the task of learning a graphical model in which the variables are of different types. For instance, we might want to reconstruct a graph for which the variables are DNA nucleotides (which take on categorical values) and gene expression measurements (which can be modeled as Gaussian, if measured using a microarray, or as Poisson, if measured using RNA-sequencing). Graphical models for mixed data, henceforth referred to as mixed graphical models, have been studied in the low-dimensional setting (Lauritzen, 1996). Recently, a few papers have considered the problem of estimating a mixed graphical model in the high-dimensional setting. Lee and Hastie (2012) proposed two algorithms for reconstructing the graph for a special case of Lauritzen’s mixed graphical model (Lauritzen, 1996), using a group lasso penalty. A less computationally intensive approach, which substitutes the group lasso penalty with an  $\ell_1$  penalty, is provided in Cheng et al. (2013). Fellinghauer et al. (2013) proposed to use random forests to estimate a mixed graphical model.

In this paper, we study mixed graphical models under a much more general setting, in which the conditional distributions of the nodes belong to the exponential family. We investigate the compatibility of such models when assuming pairwise interactions. We also study the theoretical properties of penalized estimators of this class of mixed graphical models.

## 2 A model for mixed data

We consider the pairwise graphical model (Wainwright et al., 2006), which takes the form

$$p(x) \propto \exp \left\{ \sum_{s=1}^p f_s(x_s) + \sum_{s=2}^p \sum_{t < s} f_{ts}(x_s, x_t) \right\}, \quad (1)$$

where  $x = (x_1, \dots, x_p)^T$  and  $f_{ts} = 0$  for  $\{t, s\} \notin E$ . Here,  $f_s(x_s)$  is the node potential function, and  $f_{st}(x_s, x_t)$  the edge potential function. We further simplify the pairwise interactions by assuming that  $f_{st}(x_s, x_t) = \theta_{st}x_sx_t = \theta_{ts}x_sx_t$ , so that we can write the parameters associated with edges in a symmetric square matrix  $\Theta = (\theta_{st})_{p \times p}$  where the diagonal elements equal zero. The joint density

can then be written as

$$p(x) = \exp \left\{ \sum_{s=1}^p f_s(x_s) + \frac{1}{2} \sum_{s=1}^p \sum_{t \neq s} \theta_{ts} x_s x_t - A(\Theta, \alpha) \right\}, \quad (2)$$

where  $A(\Theta, \alpha)$  is the log-partition function, a function of  $\Theta$  and  $\alpha$ , a  $K \times p$  matrix of parameters involved in the node potential functions: that is,  $f_s(x_s)$  involves  $\alpha_s$ , the  $s$ th column of  $\alpha$ . Here  $K$  is some known integer. For  $\{s, t\} \notin E$ , the edge potentials satisfy  $\theta_{st} = \theta_{ts} = 0$ . We define the neighbours of a node  $s$  as

$$N(x_s) = \{t : \theta_{ts} \neq 0\}. \quad (3)$$

Denote  $x_{-s} = (x_1, \dots, x_{s-1}, x_{s+1}, \dots, x_p)^T$ . Using the fact that  $\theta_{st} = \theta_{ts}$ , the conditional density of  $x_s | x_{-s}$  is

$$p(x_s | x_{-s}) = \exp \left\{ f_s(x_s) + \sum_{t \neq s} \theta_{ts} x_t x_s - D_s(\Theta_s, x_{-s}, \alpha_s) \right\}, \quad (4)$$

where  $D_s(\Theta_s, x_{-s}, \alpha_s)$  is a function of  $\alpha_s$ ,  $x_{-s}$ , and  $\Theta_s$ , the  $s$ th column of  $\Theta$  without the diagonal element.

Suppose  $f_s(x_s) = \alpha_{1s}x_s + \alpha_{2s}x_s^2 + \sum_{k=3}^K \alpha_{ks}B_{ks}(x_s)$ , where  $\alpha_{ks}$  is a parameter (which could be 0) and  $B_{ks}(x_s)$  is a known function ( $k = 3, \dots, K$ ). For identifiability, we assume that for  $k \geq 3$ ,  $B_{ks}(x_s)$  does not contain an additive component proportional to  $x_s$  or  $x_s^2$ . Under this assumption, (4) belongs to the exponential family. We now consider some special cases of (4), which correspond to well-known distributions previously studied in the context of graphical models (Besag 1974, Meinshausen and Bühlmann 2006, Ravikumar et al. 2010, Allen and Liu 2012, Yang et al. 2013). For convenience, we introduce a new parameter  $\eta$  defined as  $\alpha_{1s} + \sum_{t \neq s} \theta_{ts}x_t$ .

**Example 1.** The conditional density is Gaussian:

$$p(x_s | x_{-s}) = \exp \left\{ \frac{1}{2} \alpha_{2s} x_s^2 + \eta x_s + \frac{1}{2\alpha_{2s}} \eta^2 - \frac{1}{2} \log(2\pi) + \frac{1}{2} \log(-\alpha_{2s}) \right\} \quad (x_s \in \mathcal{R}), \quad (5)$$

where  $f_s(x_s) = \alpha_{1s}x_s + \alpha_{2s}x_s^2/2$  and  $D_s(\eta) = -\eta^2/(2\alpha_{2s}) - \log(-\alpha_{2s})/2 + \log(2\pi)/2$ . Assuming  $\alpha_{2s} = -1$  for simplicity, we have  $D_s(\eta) = \eta^2/2 + \log(2\pi)/2$ .

**Example 2.** The conditional density is binary. We use the coding  $x_s \in \{-1, 1\}$ , to obtain

$$p(x_s | x_{-s}) = \exp \{ \eta x_s - D_s(\eta) \}, \quad (x_s \in \{-1, 1\}), \quad (6)$$

where  $f_s(x_s) = \alpha_{1s}x_s$  and  $D_s(\eta) = \log\{\exp(\eta) + \exp(-\eta)\}$ .

**Example 3.** The conditional density is Poisson:

$$p(x_s | x_{-s}) = \exp \{ \eta x_s - \log(x_s!) - D_s(\eta) \} \quad (x_s \in \{0, 1, \dots\}), \quad (7)$$

where  $f_s(x_s) = \alpha_{1s}x_s - \log(x_s!)$  and  $D_s(\eta) = \exp(\eta)$ .

**Example 4.** The conditional density is exponential:

$$p(x_s | x_{-s}) = \exp \{ \eta x_s - D_s(\eta) \} \quad (x_s \in \mathcal{R}^+), \quad (8)$$

where  $f_s(x_s) = \alpha_{1s}x_s$  and  $D_s(\eta) = -\log(-\eta)$ .

In this paper, rather than specifying a joint distribution for all  $p$  nodes, we instead specify a conditional distribution for each node. In particular, we assume that all node-conditional distributions belong to the exponential family. We then combine the  $p$  conditional distributions to form a single graphical model, which is referred to as a conditionally-specified model (Besag, 1974; Arnold et al., 1999). This strategy has been used in prior work on estimating high-dimensional graphical models in the case where all nodes are of the same type (Meinshausen and Bühlmann, 2006; Ravikumar et al., 2010; Allen and Liu, 2012; Yang et al., 2012).

### 3 Compatibility of conditionally specified models

In this section, we consider the following question: under what circumstances does the conditionally-specified model with node-conditional distributions given in (4) correspond to a well-defined joint distribution? We adapt and restate Definition 2 in Wang and Ip (2008), which applies to any conditional density.

**Definition 1.** A non-negative function  $g$  is capable of generating a conditional density function  $p(y \mid x)$  if

$$p(y \mid x) = \frac{g(y, x)}{\int g(y, x) dy}. \quad (9)$$

Two conditional densities are said to be compatible if there exists a non-negative function  $g$  such that  $g$  is capable of generating both conditional densities. When  $g$  is a density, the conditional densities are called strongly compatible.

The following proposition shows that the conditional densities in (4) are compatible if  $\theta_{st} = \theta_{ts}$ . (The proof of Proposition 1 and other statements in this paper are available in the supplementary material.)

**Proposition 1.** Let  $x = (x_1, \dots, x_p)^\top$  be a random vector. Suppose that for each  $x_s$ , the conditional density takes the form of (4). Then, if  $\theta_{st} = \theta_{ts}$ , the following results hold: (i) The conditional densities are compatible. (ii) The function  $g$  is of the form

$$g(x) \propto \exp \left\{ \sum_{s=1}^p f_s(x_s) + \frac{1}{2} \sum_{s=1}^p \sum_{t \neq s} \theta_{ts} x_s x_t \right\}. \quad (10)$$

Under the conditions of Proposition 1, if we further assume that  $g$  is integrable, then by Definition 1, the conditional densities are strongly compatible. This proposition is closely related to Section 4.3 in Besag (1974) and Proposition 1 in Yang et al. (2012), with small modifications. For theory on compatibility of general types of conditional densities, see for example Wang and Ip (2008).

The discussion below is restricted to the case where the joint distribution, if it exists, is non-degenerate. By Proposition 1, if  $\theta_{st} = \theta_{ts}$ , then compatibility of the conditional densities given in (5)–(8) is guaranteed, provided that the conditional densities are well-defined. The following lemma makes this explicit.

Table 1: Restrictions on the parameter space required for compatibility or strong compatibility, given the conditional densities in (5)–(8)

	Gaussian	Poisson	Exponential	Binary
Gaussian	$\Theta_{JJ} \prec 0^+$	$\theta_{ts} = 0^+$	$\theta_{ts} = 0^*$	$\theta_{ts} \in \mathcal{R}$
Poisson		$\theta_{ts} \leq 0^+$	$\theta_{ts} \leq 0^{*+}$	$\theta_{ts} \in \mathcal{R}$
Exponential			$\theta_{ts} \leq 0^*$	$\sum_{s \in I}  \theta_{st}  < -\alpha_{1t}^*$
Binary				$\theta_{ts} \in \mathcal{R}$

The column specifies the type of the  $s$ th node, and the row specifies the type of the  $t$ th node. An asterisk (\*) indicates a restriction required for compatibility, and a plus (+) indicates a restriction required for strong compatibility. For compatibility to hold for a Gaussian node  $x_s$ ,  $\alpha_{2s} < 0$  is also required. Here  $\Theta_{JJ}$  is as defined in (11), and  $I$  denotes the set of binary nodes.

**Lemma 1.** *If  $\theta_{st} = \theta_{ts}$ , the necessary and sufficient conditions for the conditional densities in (5)–(8) to be compatible are as follows: (i) When  $x_s \mid x_{-s}$  is exponential,  $\theta_{ts} \leq 0$  when  $x_t$  is Poisson or exponential;  $\theta_{ts} = 0$  when  $x_t$  is Gaussian; and  $\sum_{t \in I} |\theta_{ts}| < -\alpha_{1s}$  where  $I$  denotes the index set of the binary nodes. (ii) When  $x_s \mid x_{-s}$  is Gaussian,  $\alpha_{2s} < 0$ .*

We now consider another question: Given a set of Gaussian, binary, Poisson, and exponential nodes, under what circumstances is the set of conditional distributions strongly compatible? We answer this question in the following lemma, which refers to Table 1. To help the discussion, we introduce some notation for the Gaussian nodes. Suppose that  $J$  indexes the Gaussian nodes: i.e. for  $s \in J$ ,  $x_s \mid x_{-s}$  is Gaussian. Without loss of generality, suppose that the nodes are ordered such that  $J = (1, \dots, m)$ . We define a matrix  $\Theta_{JJ}$  as

$$\Theta_{JJ} = \begin{pmatrix} \alpha_{21} & \theta_{12} & \cdots & \theta_{1m} \\ \theta_{21} & \alpha_{22} & \cdots & \theta_{2m} \\ \vdots & \vdots & \ddots & \vdots \\ \theta_{m1} & \theta_{m2} & \cdots & \alpha_{2m} \end{pmatrix}. \quad (11)$$

**Lemma 2.** *If  $\theta_{st} = \theta_{ts}$ , the conditions in Table 1 are necessary and sufficient for the conditional densities in (5)–(8) to be strongly compatible.*

Table 1 reveals the limitations for compatibility and strong compatibility of the conditionally-specified model. For example, only negative associations between an exponential node and a Poisson or exponential node can be captured, and no associations between Gaussian nodes and Poisson or exponential nodes can be captured.

As discussed, given that the conditional densities are in the form of (5)–(8), existence of the joint density imposes substantial constraints on the parameter space, and thus limits the flexibility of the resulting conditionally-specified model. In this paper, rather than modeling the joint distribution, we instead model the node-conditional distributions directly as in (5)–(8). In this way, we are able to overcome some of the inherent limitations of the joint density.

## 4 Estimation Via Neighbourhood Selection

Our goal is to recover the structure of the graph from a set of observations. We take the approach of maximizing penalized conditional likelihoods node-by-node, using a neighbourhood selection approach. A similar approach has been studied in univariate exponential family settings, such as Gaussian, binary, and Poisson (Meinshausen and Bühlmann, 2006; Ravikumar et al., 2010; Yang et al., 2012).

Recall that  $f_s(x_s) = \alpha_{1s}x_s + \alpha_{2s}x_s^2 + \sum_{k=3}^K \alpha_{ks}B_{ks}(x_s)$ . We now simplify the problem further by assuming that  $\alpha_{ks}$  is known for any  $k \geq 2$ . From now on, we use an asterisk (\*) to denote the true parameter values. Let  $X$  denote a  $n \times p$  data matrix, with the  $i$ th row given by  $x^{(i)}$ . We estimate  $\Theta_s^*$  and  $\alpha_{1s}^*$  with

$$\underset{\Theta_s \in \mathcal{R}^{p-1}, \alpha_{1s} \in \mathcal{R}}{\text{minimize}} \quad -\ell_s(\Theta_s, \alpha_{1s}; X) + \lambda_n \|\Theta_s\|_1, \quad (12)$$

where

$$\ell_s(\Theta_s, \alpha_{1s}; X) = \frac{1}{n} \sum_{i=1}^n \log p(x_s^{(i)} | x_{-s}^{(i)});$$

the conditional density  $p(x_s^{(i)} | x_{-s}^{(i)})$  is defined in (4). Note that in (12) we do not penalize  $\alpha_{1s}$ . (12) is a convex problem with respect to  $(\Theta_s^T, \alpha_{1s})^T$  since the log-likelihood is convex given the form of (4). For instance, if  $x_s$  is Gaussian, then (12) amounts to an  $\ell_1$ -penalized linear regression, and if  $x_s$  is binary, then it amounts to an  $\ell_1$ -penalized logistic regression. Finally, we let the estimated neighbourhood of  $x_s$  be

$$\hat{N}(x_s) = \{t : \hat{\theta}_{ts} \neq 0\}, \quad (13)$$

where  $\hat{\Theta}_s$  solves (12), and  $\hat{\theta}_{ts}$  is the element corresponding to an edge with the  $t$ th node.

In practice, in order to avoid a situation in which the variables are on different scales, we may wish to modify (12) in order to allow a different weight for the  $\ell_1$ -penalty on each coefficient. We define a weight vector  $w$  equal to the empirical standard errors of the corresponding variables:  $w = (\hat{\sigma}_1, \dots, \hat{\sigma}_{s-1}, \hat{\sigma}_{s+1}, \dots, \hat{\sigma}_p)^T$ , and let the penalty term be  $\lambda_n \|w^T \Theta_s\|_1$  instead of  $\lambda_n \|\Theta_s\|_1$  in (12), i.e.

$$\underset{\Theta_s \in \mathcal{R}^{p-1}, \alpha_{1s} \in \mathcal{R}}{\text{minimize}} \quad -\ell_s(\Theta_s, \alpha_{1s}; X) + \lambda_n \|w^T \Theta_s\|_1. \quad (14)$$

The weighted version (14) is preferred in practice (Lee and Hastie, 2012), though in our theoretical analysis we stick with (12) for simplicity. The convex problems (12) and (14) can be easily solved using existing algorithms (e.g. Friedman et al. 2010).

In the joint density (2), the parameter matrix  $\Theta$  is symmetric, i.e.  $\theta_{st} = \theta_{ts}$ . But the neighbourhood selection method does not guarantee symmetric estimates, and the estimated neighbourhoods might not match: for instance, it could happen that  $\hat{\theta}_{st} = 0$  but  $\hat{\theta}_{ts} \neq 0$ . Our analysis in Section 5.2 shows that we can exploit the asymmetry in  $\hat{\theta}_{st}$  and  $\hat{\theta}_{ts}$  when  $x_s$  and  $x_t$  are of different types, in order to obtain more efficient edge estimates.

## 5 Theoretical results

### 5.1 Neighbourhood recovery when the joint density exists

In this subsection we show that if the joint density exists for the conditional densities in (4) (as it will under conditions discussed in Section 3), then under some additional assumptions, the true neighbourhood is consistently selected using the proposed neighbourhood selection approach. Here we rely heavily on results from Yang et al. (2013), who consider a related problem in which all nodes have the same distribution.

In the following discussion, we assume that  $p > n$  for simplicity. For any  $s$ , let  $\Delta_s$  denote the set of indices for elements of  $(\Theta_s^T, \alpha_{1s})^T$  that correspond to non-neighbours of the  $s$ th node, and let  $Q_s^* = -\nabla^2 \ell_s(\Theta_s^*, \alpha_{1s}^*; X)$  be the negative Hessian of  $\ell_s(\Theta_s, \alpha_{1s}; X)$  with respect to  $(\Theta_s^T, \alpha)^T$ . Below we suppress the subscript  $s$  for simplicity, and we remind the reader that all quantities are related to the node-wise density. We express  $Q^*$  in blocks:

$$Q^* = \begin{pmatrix} Q_{\Delta^c \Delta^c}^* & Q_{\Delta^c \Delta}^* \\ Q_{\Delta \Delta^c}^* & Q_{\Delta \Delta}^* \end{pmatrix}.$$

The first two assumptions are about the sample information matrix of the node-conditional distribution.

**Assumption 1.** (The irrepresentability assumption) There exists a positive number  $a$  such that

$$\max_{l \in \Delta} \|Q_{l \Delta^c}^* (Q_{\Delta^c \Delta^c}^*)^{-1}\|_1 \leq 1 - a.$$

The irrepresentability assumption is common for variable selection consistency of  $\ell_1$ -penalized regression. The intuition is that the non-neighbours should not exert too much effect on the neighbours.

**Assumption 2.** (The dependency assumption) The eigenvalues of  $Q_{\Delta^c \Delta^c}^*$  are bounded from below by some positive number  $\Lambda_1$ . That is, there exists  $\Lambda_1 > 0$  such that  $\Lambda_{\min}(Q_{\Delta^c \Delta^c}^*) \geq \Lambda_1$ . Also, there exists  $\Lambda_2 < \infty$  such that  $\Lambda_{\max} \left( \sum_{i=1}^n x_0^{(i)} (x_0^{(i)})^T / n \right) \leq \Lambda_2$  where  $x_0 = (x_{-s}^T, 1)^T$ .

The next assumption is on the derivatives of the log-partition function  $D$  in (4). The log-partition function plays a key role in bounding the tails since it is closely related to the cumulant generating function.

**Assumption 3.** The log-partition function of the conditional density  $p_s$  is third-order differentiable, and there exist  $\kappa_2$  and  $\kappa_3$  such that  $|D''(\eta)| \leq \kappa_2$  and  $|D'''(\eta)| \leq \kappa_3$  for  $\eta \in \{\eta : \eta \in \mathcal{D}, |\eta| \leq M\delta_1 \log p\}$ , where  $\mathcal{D}$  is the support of  $D(\cdot)$ .

*Remark 1.*  $\kappa_2$  and  $\kappa_3$  are functions of  $p$ . The quantity  $\delta_1$  is a constant to be chosen in Proposition 2.  $M$  is a sufficiently large constant that plays a role in Condition 2.

Recall that the parameter  $\eta$  equals  $\alpha_{1s} + \sum_{t \neq s} \theta_{ts} x_t$ , so there is a need to bound  $\sum_{t \neq s} \theta_{ts} x_t$  in order for Assumption 3 to be practical. Using properties of the exponential family, we are able to derive concentration inequalities for  $x_s$ , given the following assumptions on the first and second moments of  $x_s$  and on  $A$  in the joint distribution (2).

**Assumption 4.** Assume that, for  $t = 1, \dots, p$ , (i)  $|E(x_t)| \leq \kappa_m$ , (ii)  $E(x_t^2) \leq \kappa_v$ , and (iii)

$$\max_{u:|u|\leq 1} \left. \frac{\partial^2 A}{\partial \alpha_{1t}^2} \right|_{\alpha_{1t}^*+u} \leq \kappa_h, \quad \max_{u:|u|\leq 1} \left. \frac{\partial^2 A}{\partial \alpha_{2t}^2} \right|_{\alpha_{2t}^*+u} \leq \kappa_h.$$

Given Assumption 4, the following propositions on the marginal behaviour of random variables hold (see Propositions 2 and 3 in Yang et al. 2013).

**Proposition 2.** Define the event

$$\xi_1 = \left[ \max_{i \in \{1, \dots, n\}; t \in \{1, \dots, p\}} \{|x_t^{(i)}|\} < \delta_1 \log p \right].$$

Assuming  $p > n$ ,  $\text{pr}(\xi_1) \geq 1 - c_1 p^{-\delta_1+2}$ , where  $c_1 = \exp(\kappa_m + \kappa_h/2)$ .

**Proposition 3.** Define the event

$$\xi_2 = \left[ \max_{t \in \{1, \dots, p\}} \left\{ \frac{1}{n} \sum_{i=1}^n (x_t^{(i)})^2 \right\} < \delta_2 \right],$$

where  $\delta_2 \geq 1$ . If  $\delta_2 \leq \min\{2\kappa_v/3, \kappa_h + \kappa_v\}$ , and  $n \geq 8\kappa_h^2 \log p / \delta_2^2$ , then  $\text{pr}(\xi_2) \geq 1 - \exp\{-c_2 \delta_2^2 n\}$ , where  $c_2 = 1/(4\kappa_h^2)$ .

Assumptions 1 to 4 lay the foundation for neighbourhood selection consistency. We also need three extra conditions related to penalized regression.

**Condition 1.** The minimum of edge potentials related to node  $x_s$ ,  $\min_{t \in N(x_s)} \{|\theta_{ts}|\}$ , is larger than  $10(d+1)^{1/2} \lambda_n / \Lambda_1$ , where  $d$  is the number of neighbours of  $x_s$ .

**Condition 2.** The tuning parameter  $\lambda_n$  is in the range

$$\left[ \frac{8(2-a)}{a} \left\{ \delta_2 \kappa_2 \frac{\log(2p)}{n} \right\}^{1/2}, \min \left\{ \frac{2(2-a)}{a} \kappa_2 \delta_2 M, \frac{a \Lambda_1^2 (d+1)^{-1}}{288(2-a) \kappa_2 \Lambda_2}, \frac{\Lambda_1^2 (d+1)^{-1}}{12 \Lambda_2 \kappa_3 \delta_1 \log p} \right\} \right]. \quad (15)$$

*Remark 2.* Of the three quantities in the upper bound of  $\lambda_n$ ,  $\Lambda_1^2 / \{12 \Lambda_2 (d+1) \kappa_3 \delta_1 \log p\}$  is usually the smallest because of the  $\log p$  in the denominator.

**Condition 3.** The sample size  $n$  is no smaller than  $8\kappa_h^2 \log p / \delta_2^2$ , and also the range of feasible  $\lambda_n$  in Condition 2 is not empty, i.e.

$$n \geq \frac{96^2 (2-a)^2 \Lambda_2^2}{a^2 \Lambda_1^4} (d+1)^2 \kappa_2 \kappa_3^2 \delta_1^2 \delta_2 \log(2p) (\log p)^2. \quad (16)$$

**Theorem 1.** Suppose that the joint density (2) exists and Assumption 4 holds. For any given  $s$ , suppose Assumptions 1, 2, and 3 hold, and Conditions 1, 2, and 3 are met. Then with probability at least  $1 - c_1 p^{-\delta_1+2} - \exp(-c_2 \delta_2^2 n) - \exp(-c_3 \delta_3 n)$ , for some constants  $c_1, c_2, c_3$ ,  $\delta_2 \leq \min\{2\kappa_v/3, \kappa_h + \kappa_v\}$ , and  $\delta_3 = 1/(\kappa_2 \delta_2)$ , the solution of (12) recovers the true neighbourhood exactly, so that  $\hat{N}(x_s) = N(x_s)$ .



Theorem 1 shows that the probability of successful recovery increases exponentially with  $n$ , when  $n$  is greater than the minimum sample size required by Conditions 3. Noting that the number of neighbours  $d$  appears in Conditions 1, 2, and 3, we need the true graph  $G$  to be sparse (i.e.  $d = o(n)$ ) in order for Theorem 1 to be meaningful.

The quantities  $\delta_2\kappa_2$  and  $\delta_1\kappa_3$  appear in the upper bound of  $\lambda_n$  (15) and the minimum sample size (16). The fact that  $\kappa_2$  and  $\delta_2$  appear together in a product implies that we can relax the restriction on  $\delta_2$  if  $\kappa_2$  is small. The same applies to  $\delta_1$  and  $\kappa_3$ .

For certain types of nodes, Theorem 1 holds with a less stringent set of assumptions and conditions. For a Gaussian node, specifically, the second-and-higher order derivatives of  $D(\eta)$  are always bounded, i.e.  $\kappa_2 = 1$  and  $\kappa_3 = 0$ . The fact that  $D'''(\eta) = 0$  has profound effects on the theory, as illustrated in Corollary 1 below.

**Corollary 1.** *Suppose that the joint density (2) exists and Assumption 4 holds. For any given  $s$ , Assumptions 1, 2, and 3 and Condition 1 hold, and*

$$\lambda_n \in \left[ \frac{8(2-a)}{a} \left\{ \delta_2\kappa_2 \frac{\log(2p)}{n} \right\}^{1/2}, \frac{2(2-a)}{a} \kappa_2\delta_2 M \right], \quad n \geq \frac{8\kappa_h^2 \log p}{\delta_2^2}.$$

*Then with probability at least  $1 - \exp(-c_2\delta_2^2n) - \exp(-c_3\delta_3n)$ , for some constants  $c_2, c_3$ ,  $\delta_2 \leq \min\{2\kappa_v/3, \kappa_h + \kappa_v\}$ , and  $\delta_3 = 1/(\kappa_2\delta_2)$ , the solution of (12) recovers the true neighbourhood exactly, so that  $\hat{N}(x_s) = N(x_s)$ .*

## 5.2 Combining Neighbourhoods to Estimate the Edge Set

The neighbourhood selection approach may give asymmetric estimates, in the sense that  $t \in \hat{N}(x_s)$  but  $s \notin \hat{N}(x_t)$ . To deal with this discrepancy, two strategies for estimating a single edge set were proposed in Meinshausen and Bühlmann (2006), and adapted in other work:

$$\begin{aligned} \hat{E}_{\text{and}} &= \left[ \{s, t\} : s \in \hat{N}(x_t) \text{ and } t \in \hat{N}(x_s) \right], \\ \hat{E}_{\text{or}} &= \left[ \{s, t\} : s \in \hat{N}(x_t) \text{ or } t \in \hat{N}(x_s) \right]. \end{aligned}$$

When the  $s$ th and  $t$ th nodes are of the same type, there is no clear reason to prefer the edge estimate from  $\hat{N}(x_s)$  over the one from  $\hat{N}(x_t)$ , and so the choice of  $\hat{E}_{\text{and}}$  versus  $\hat{E}_{\text{or}}$  is not crucial (Meinshausen and Bühlmann, 2006). When the  $s$ th and  $t$ th nodes are of different types, however, the choice matters. We now take a closer look at this issue with examples of Gaussian, binary, exponential and Poisson nodes as in (5)–(8). Quantities  $c_1$ ,  $c_2$ , and  $c_3$  in Theorem 1 are the same regardless of the node type, while the values of  $\delta_1$  and  $\delta_2$  can change depending on the type of node being regressed on the others in (12). Thus, we consider the values of  $\delta_1$  and  $\delta_2$  and hence the implications of Theorem 1 for each node type. We fix  $B_1 = \kappa_3\delta_1$  for binary, Poisson and exponential nodes. For a Gaussian node, this quantity will always equal zero, since  $D(\eta) = \eta^2/2 + \log(2\pi)/2$  and hence  $D'''(\eta) = 0 = \kappa_3$ . Furthermore, we fix  $B_2 = 1/\delta_3 = \delta_2\kappa_2$  for all four types of nodes. With  $B_1$  and  $B_2$  fixed, the minimum sample size and the feasible range of the tuning parameter for binary, Poisson and exponential nodes are exactly the same, and they are more restrictive than the corresponding values for Gaussian nodes given in Corollary 1. In the following,  $N_G$ ,  $N_B$ ,  $N_P$ , and  $N_E$  denote the neighbourhoods of a Gaussian, binary, Poisson, and exponential node, respectively.

**Example 5.** For a Gaussian node, the log-partition function is  $D(\eta) = \eta^2/2 + \log(2\pi)/2$ . It follows that  $D''(\eta) = 1 = \kappa_2$ . Thus,  $\delta_2 = B_2$ . As discussed in Corollary 1, the feasible range of  $\lambda_n$  is  $[8(2-a)\{\log(2p)B_2/n\}^{1/2}/a, 2(2-a)B_2M/a]$  and the minimum sample size is  $8\kappa_h^2 \log p/B_2^2$ . A lower bound for the probability of successful neighbourhood recovery is

$$\text{pr}(\hat{N}_G = N_G) \geq 1 - \exp(-c_2 B_2^2 n) - \exp(-c_3 n/B_2). \quad (17)$$

**Example 6.** For a binary node, the log-partition function of the conditional density is  $D(\eta) = \log\{\exp(-\eta) + \exp(\eta)\}$ , so that  $|D''(\eta)| \leq 1$  and  $|D'''(\eta)| \leq 2$ . Consequently,  $\delta_2 = B_2$ , and  $\delta_1 = B_1/\kappa_3 = B_1/2$ . From Condition 2, the range of feasible  $\lambda_n$  is  $[8(2-a)\{\log(2p)B_2/n\}^{1/2}/a, \Lambda_1^2/\{12\Lambda_2(d+1)B_1 \log p\}]$ . From Condition 3, the minimum sample size is  $96^2(2-a)^2\Lambda_2^2(d+1)^2B_2B_1^2 \log(2p)(\log p)^2/(a^2\Lambda_1^4)$ . By Theorem 1, a lower bound for the probability of successful neighbourhood recovery is

$$\text{pr}(\hat{N}_B = N_B) \geq 1 - c_1 p^{-B_1/2+2} - \exp(-c_2 B_2^2 n) - \exp(-c_3 n/B_2). \quad (18)$$

**Example 7.** For a Poisson node, the log-partition function is  $D(\eta) = \exp(\eta)$ , so  $D''(\eta) = D'''(\eta) = \exp(\eta)$ . To bound  $D''(\eta)$  and  $D'''(\eta)$ , we need to bound  $\exp(\eta)$ . Recall from Table 1 that strong compatibility requires that  $\theta_{ts}x_t \leq 0$  when  $x_t$  is Gaussian, Poisson or exponential. Therefore, an upper bound of  $\exp(\eta)$  is

$$\exp(\eta) \leq \exp\left(\alpha_{1s} + \sum_{t \in I} |\theta_{ts}|\right) \equiv b_P, \quad (19)$$

where  $I$  is the set of binary nodes. Therefore,  $\kappa_2 = \kappa_3 = b_P$ , and so  $\delta_2 = B_2/b_P$  and  $\delta_1 = B_1/b_P$ . The range of feasible  $\lambda_n$  and the minimum sample size are the same as for a binary node, as these quantities involve only  $B_1$  and  $B_2$ , which are fixed. A lower bound on the probability of successful neighbourhood recovery is

$$\text{pr}(\hat{N}_P = N_P) \geq 1 - c_1 p^{-\frac{B_1}{b_P}+2} - \exp(-c_2 B_2^2 n/b_P^2) - \exp(-c_3 n/B_2). \quad (20)$$

**Example 8.** For an exponential node, the log-partition function is  $D(\eta) = -\log(-\eta)$ , so  $D''(\eta) = \eta^{-2}$  and  $D'''(\eta) = -2\eta^{-3}$ . Recall from Table 1 that in order for the conditional density to be well-defined,  $\theta_{ts}x_t \leq 0$  when  $x_t$  is Gaussian, Poisson or exponential. Consequently,

$$\eta = \alpha_{1s} + \sum_{t \neq s} \theta_{ts}x_t \geq \alpha_{1s} + \sum_{t \in I} \theta_{ts}x_t,$$

where  $I$  is the set of binary nodes. It follows that

$$|\eta| \geq |\alpha_{1s}| - \sum_{t \in I} |\theta_{ts}x_t| = |\alpha_{1s}| - \sum_{t \in I} |\theta_{ts}| \equiv b_E. \quad (21)$$

As a result,  $|D''(\eta)|$  and  $|D'''(\eta)|$  are bounded by  $\kappa_2 = b_E^{-2}$  and  $\kappa_3 = 2b_E^{-3}$ , respectively. For fixed  $B_1$  and  $B_2$ , we have  $\delta_2 = b_E^2 B_2$  and  $\delta_1 = B_1 b_E^3/2$ . The range of feasible  $\lambda_n$  and the minimum sample size are the same as for a binary node, as these quantities involve only  $B_1$  and  $B_2$ , which are fixed. A lower bound for the probability of successful neighbourhood recovery is

$$\text{pr}(\hat{N}_E = N_E) \geq 1 - c_1 p^{-b_E^3 B_1/2+2} - \exp(-c_2 b_E^4 B_2^2 n) - \exp(-c_3 n/B_2). \quad (22)$$

Examples 5-8 reveal that the neighbourhood of a Gaussian node is easier to recover than the neighbourhood of the other three types of nodes: Gaussian node recovery requires a smaller minimum sample size, allows for a wider range of feasible tuning parameters, and has (in general) a higher probability of success. As a result, the neighbourhood of the Gaussian node should be used when estimating an edge between a Gaussian node and a non-Gaussian node.

Which neighbourhood should we use to estimate an edge between two non-Gaussian nodes? In this setting, there are no clear winners, because while (18) can be evaluated given knowledge of  $c_1$ ,  $c_2$ , and  $c_3$ , (20) and (22) also require knowledge of the unknown quantities  $b_E$  and  $b_P$ , which are functions of unknown quantities  $\Theta_s$  and  $\alpha_{1s}$  (Equations 19 and 21). One possibility is to plug in a consistent estimator for these parameters (see e.g. Van de Geer 2008, Bunea 2008, van de Geer et al. 2013) in order to obtain a consistent estimator for  $b_P$  or  $b_E$ . This leads to the following lemma.

**Lemma 3.** *Suppose  $\tilde{\Theta}_s$  and  $\tilde{\alpha}_{1s}$  are consistent estimators for the true parameters in the conditional densities (7) and (8). Let  $I$  be the index set of the binary nodes. The following are consistent estimators of the probability of successful neighbourhood recovery:*

1. *For a Poisson node, let  $\tilde{b}_P = \exp(\tilde{\alpha}_{1s} + \sum_{t \in I} |\tilde{\theta}_{ts}|)$ . Then, the estimator for the probability of successful neighbourhood recovery is*

$$1 - c_1 p^{-B_1/\tilde{b}_P+2} - \exp(-c_2 B_2^2 n / \tilde{b}_P^2) - \exp(-c_3 n / B_2). \quad (23)$$

2. *For an exponential node, let  $\tilde{b}_E = |\tilde{\alpha}_{1s}| - \sum_{t \in I} |\tilde{\theta}_{ts}|$ . Then, the estimator for the probability of successful neighbourhood recovery is*

$$1 - c_1 p^{-\tilde{b}_E^3 B_1/2+2} - \exp(-c_2 \tilde{b}_E^4 B_2^2 n) - \exp(-c_3 n / B_2). \quad (24)$$

Therefore, by plugging in consistent estimators of  $\Theta_s$  and  $\alpha_{1s}$  into (19) or (21), we can reconstruct an edge by choosing the neighbourhood for which the probability of correct recovery is highest (according to (17), (18), (23), and (24)). The rules are summarized in Table 2. In a sense, the results in this section illustrate a worst case scenario for recovery of each neighbourhood, in that Theorem 1 provides a lower bound for the probability of successful neighbourhood recovery.

## 6 Neighbourhood recovery and selection without a proper joint density

In Section 5, we discussed the situation in which the joint density is well-defined. However, for an arbitrary set of node-conditional distributions, a joint density capable of generating the conditional densities in (4) may not exist. In contrast, here we show that one can always recover the neighbours of a single node using node-wise regression. When no joint density is available, we define the neighbourhood of  $x_s$  based upon its conditional density, (4) as

$$N^0(x_s) = \{t : \tilde{\theta}_{ts} \neq 0\}, \quad (\tilde{\Theta}_s^T, \tilde{\alpha}_{1s})^T = \underset{\Theta_s \in \mathcal{R}^{p-1}, \alpha_{1s} \in \mathcal{R}}{\operatorname{argmax}} E[\log p(x_s | x_{-s})]. \quad (25)$$

Table 2: Neighbourhood to use in estimating an edge between two non-Gaussian nodes of different types

	Selection rules
Poisson & Exponential	Choose Poisson if $\tilde{b}_E^2 \tilde{b}_P < 1$ and $\tilde{b}_E^3 \tilde{b}_P < 2$ . Choose exponential if $\tilde{b}_E^2 \tilde{b}_P > 1$ and $\tilde{b}_E^3 \tilde{b}_P > 2$ .
Poisson & Binary	Choose Poisson if $\tilde{b}_P < 1$ . Choose binary if $\tilde{b}_P > 2$ .
Exponential & Binary	Choose exponential if $\tilde{b}_E \geq 1$ . Choose binary if $\tilde{b}_E < 1$ .

When the conditions are not met, there is no clear preference.

Here  $\tilde{\theta}_{ts}$  is the element of  $\tilde{\Theta}_s$  that corresponds to an edge with the  $t$ th node. When the joint density exists, the definitions (3) and (25) are equivalent, because  $\Theta_s^*$  and  $\alpha_{1s}^*$  maximize  $E[\log p(x_s | x_{-s})]$ .

Assumption 4 is no longer appropriate in the absence of a joint density. Therefore, we make the following assumption to replace Propositions 2 and 3.

**Assumption 5.** Assume that (i)  $\text{pr}(\xi_1) \geq 1 - c_1 p^{-\delta_1+2}$ , (ii)  $\text{pr}(\xi_2) \geq 1 - \exp\{-c_2 \delta_2^2 n\}$ .

We arrive at the following theorem.

**Theorem 2.** Suppose that the  $s$ th node has conditional density (4), and suppose that Assumptions 1, 2, 3, and 5 hold. Furthermore, suppose that Conditions 1, 2 and 3 are met. Then with probability at least  $1 - c_1 p^{-\delta_1+2} - \exp(-c_2 \delta_2^2 n) - \exp(-c_3 \delta_3 n)$ , for some constants  $c_1, c_2, c_3$ , and  $\delta_3 = 1/(\kappa_2 \delta_2)$ , the solution to (12) recovers the true neighbourhood exactly, so that  $\hat{N}(x_s) = N^0(x_s)$ .

The proof of Theorem 2 is similar to that of Theorem 1, and is thus omitted. The only difference between the conclusions of Theorems 1 and 2 involves the use of  $N^0(x_s)$  instead of  $N(x_s)$ . Theorem 2 indicates that our neighbourhood selection approach can recover the neighbourhood defined in (25) exactly, regardless of whether a joint density capable of generating the conditional densities in (4) exists. Consequently, we can model relationships between nodes that are far more flexible than those outlined in Table 1.

Furthermore, Theorem 2 enables us to extend the discussion in Section 5.2. For Gaussian, binary, and exponential nodes, that discussion did not require the existence of a joint density, and so the probabilities of successful recovery derived in that section (Equations 17, 18, and 24) apply here directly. In contrast, the results for the Poisson node (Equation 23) relied on the fact that under the conditions for existence of a joint density given in Table 1,  $\tilde{b}_P$  as defined in the statement of Lemma 3 is a consistent estimator of the upper bound of  $\exp(\eta)$ . Consequently, (23) does not apply in the absence of a joint density. We leave as a topic for future work the derivation of analogous selection rules for a Poisson node in the case where the joint density does not exist.

## 7 Simulation study

### 7.1 Data generation

We consider a mixed graphical model consisting of  $m = p/2$  binary and  $m = p/2$  Gaussian nodes (Lauritzen, 1996; Lee and Hastie, 2012); without loss of generality, we order the nodes so that the Gaussian ones precede the binary ones. We construct a graph in which each node is connected with the adjacent nodes of the same type, and also the  $j$ th Gaussian node is connected with the  $j$ th binary node, for  $j = 1, \dots, m$ . As a result, all nodes have three neighbours, except for the first and  $m$ th Gaussian nodes and the first and  $m$ th binary nodes.

Based on the edge set  $E$  defined in the previous paragraph, we generate a matrix  $\Theta$  that has non-zero elements on the edges. First, we draw a  $p \times p$  matrix  $T$ , with diagonal elements equal to 1,  $T_{ij} = 0$  for  $\{i, j\} \notin E$ , and

$$T_{ij} = T_{ji} = y_{ij}r_{ij}, \quad \text{pr}(y_{ij} = \pm 1) = 0.5, \quad r_{ij} \sim \text{Unif}(a, b) \quad (\{i, j\} \in E, \quad i < j), \quad (26)$$

where  $a$  and  $b$  are two positive numbers to be specified. We then let  $\tilde{T} = T$ , except for  $\tilde{T}_{(1:m) \times (1:m)}$ , which is defined as  $\tilde{T}_{(1:m) \times (1:m)} = -\{T_{(1:m) \times (1:m)} - \Lambda_{\min}(T_{(1:m) \times (1:m)}) + 0.1I_{m \times m}\}$ ; this guarantees that  $\tilde{T}_{(1:m) \times (1:m)}$  is negative definitive as required in Table 1. We standardize  $\tilde{T}$  as

$$\tilde{T} = \text{diag}(|\tilde{T}_{11}|^{-1/2}, \dots, |\tilde{T}_{pp}|^{-1/2}) \tilde{T} \text{diag}(|\tilde{T}_{11}|^{-1/2}, \dots, |\tilde{T}_{pp}|^{-1/2}).$$

Finally, we let  $\theta_{ij} = \tilde{T}_{ij}$  for  $i \neq j$  and  $\theta_{ii} = 0$  ( $i = 1, \dots, p$ ). Recall that we have assumed that  $f_s(x_s) = \alpha_{1s}x_s + \alpha_{2s}x_s^2 + \sum_{k=3}^K \alpha_{ks}B_{ks}(x_s)$  in (2): we set  $\alpha_{2s} = \tilde{T}_{ss}$  ( $s = 1, \dots, m$ ),  $\alpha_{2s} = 0$  ( $s = m+1, \dots, p$ ), and  $\alpha_{ks} = 0$  for  $k \neq 2$ .

To draw samples from the joint density  $p(x)$ , we employed a Gibbs sampler, as used in Lee and Hastie (2012). Briefly, we obtain the distribution of the binary nodes by integrating over the Gaussian nodes in (2), and then use a Gibbs sampler to draw random samples from  $p(x_{(m+1):2m})$ . We set the burn-in to be 3000, and take one observation every 500 draws to preserve independence. Given  $x_{(m+1):2m}$ , we draw the Gaussian nodes  $x_{1:m}$  from the conditional distribution  $p(x_{1:m} \mid x_{(m+1):2m})$ .

### 7.2 Probability of successful neighbourhood recovery

In Section 5.2 we saw that the probability of successful neighbourhood recovery depends on the type of node. In particular, the estimates from the Gaussian nodes are more reliable than the ones from binary nodes. We now verify those findings by studying the empirical probability of successful neighbourhood recovery of a graph or a sub-graph in simulations. Here, successful neighbourhood recovery is defined to mean that the estimated edge set of a graph or a sub-graph is exactly the same as the true edge set. The probabilities and minimum sample sizes for successful neighbourhood recovery are highly dependent on the parameter matrix  $\Theta$  in (2), which determines the constants  $c_1, c_2$  and  $c_3$  in Theorem 1. For simplicity, we set  $a = b = 0.3$  in (26), and generate one graph for each of  $p = 60$ ,  $p = 120$ , and  $p = 240$ . For each graph, 100 independent data sets are drawn from the Gibbs sampler. In applying our neighbourhood selection procedure, we set the tuning parameter  $\lambda_n$  to be a constant  $c$  times  $\{\log(p)/n\}^{1/2}$ , so that it is on the scale required by Theorem 1. We obtain the estimator by solving the weighted optimization problem (14).

Figure 1 displays the probability of successful neighbourhood recovery. For ease of viewing, we display the empirical probability curves separately for the Gaussian-Gaussian, binary-binary, and binary-Gaussian subgraphs. Panels (a) and (b) are estimates obtained by regressing the Gaussian nodes onto the others, and panels (c) and (d) are the estimates from regressing the binary nodes onto the others. The results are consistent with the inference in Section 5.2: the recovery of the neighbourhood of a Gaussian node requires smaller minimum sample sizes and enjoys a higher probability of successful neighbourhood recovery than that of a binary node.

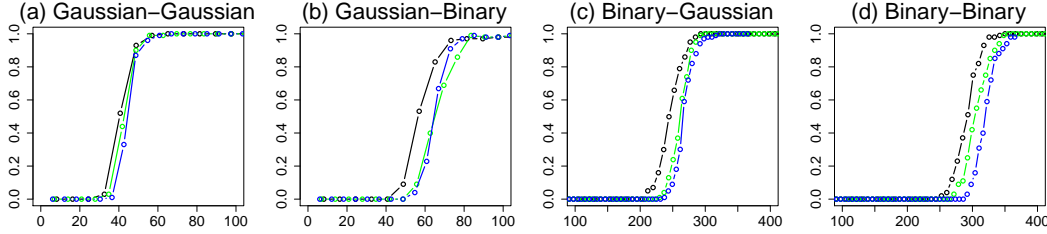


Figure 1: Probability of successful neighbourhood recovery ( $y$ -axis) as a function of the scaled sample size  $n / \{3 \log(p)\}$  ( $x$ -axis). The three curves are empirical probabilities of successful neighbourhood recovery for graphs with 60 nodes (—), 120 nodes (—), and 240 nodes (—). Estimates are averaged over 100 independent data sets. The tuning parameter is set to be  $2.6 \{\log(p)/n\}^{1/2}$ . The title of each panel indicates the subgraph for which the recovery probability is displayed, and the node on the left in the title indicates the node type that was regressed in order to obtain the subgraph estimate. For instance, panel (b) displays probability curves for edges between Gaussian and binary nodes that are estimated from the  $\ell_1$ -penalized linear regression of Gaussian nodes. Panel (c) displays the same quantity, estimated via an  $\ell_1$ -penalized regression of the binary nodes.

### 7.3 Comparison to competing approaches

In this section, we investigate the following question: is there a practical benefit (in terms of edge selection) to estimating a graph containing mixed nodes using our proposed approach, rather than simply assuming that all nodes are of the same type? We generate 100 random graphs with  $p = 40$ , and with  $a = 0.3$  and  $b = 0.6$  in (26). 20 independent samples are generated from each graph using the Gibbs sampler. Each sample contains  $n = 200$  observations. We evaluate the performance of each approach by computing (a) Kendall's  $\tau$  rank correlation between the true edges and their estimated values, and (b) the number of true positive estimated edges. Both are averaged over 2000 simulated data sets (20 for each of the 100 random graphs).

Four algorithms are compared in the study: 1) our proposal for neighbourhood selection in the mixed graphical model; 2) neighbourhood selection in the Gaussian graphical model (Meinshausen and Bühlmann, 2006), where we use  $\ell_1$ -penalized linear regression on all nodes; 3) the graphical lasso (Friedman et al., 2008), which treats all features as Gaussian; and 4) neighbourhood selection in the Ising model (Ravikumar et al., 2010), where we use  $\ell_1$ -penalized logistic regression on all nodes after dichotomizing the Gaussian nodes by their means.

Results are shown in Figure 2. In general, our proposal for neighbourhood selection in the mixed graphical model performs better than the competitors, which is expected since it assumes

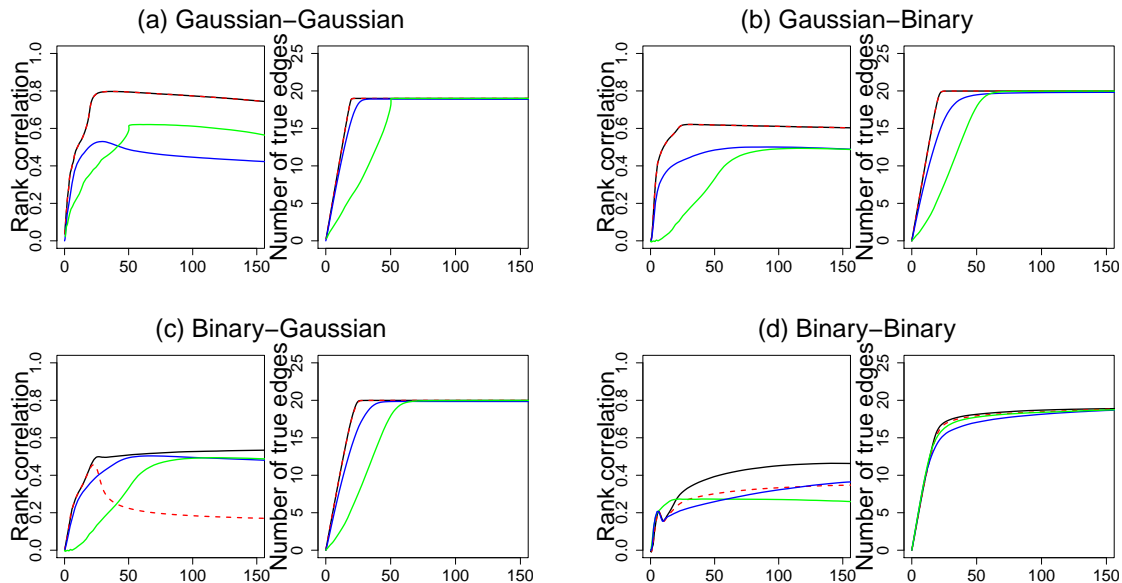


Figure 2: Edge selection efficiency of four algorithms on a sample of size 200 for a graph with 40 nodes. The  $x$ -axis displays the number of estimated edges. Within each panel, the curves represent our proposal for neighbourhood selection in the mixed graphical model (—), neighbourhood selection in the Gaussian graphical model (---), neighbourhood selection in the Ising model (—), and the graphical lasso (—). The four panels are titled using the conventions described in the caption for Figure 1. For instance, panel (c) shows edge selection results for the binary-Gaussian subgraph, with edges estimated via a regression of the binary nodes on the others.

the correct model. Neighbourhood selection in the Gaussian graphical model shows similar performance to the proposed method in terms of edge selection: in fact, neighbourhood selections in the Gaussian graphical model and in the mixed graphical model yield identical results in panels (a) and (b), in which Gaussian nodes are regressed upon the others. But neighbourhood selection in the Gaussian graphical model performs far worse in terms of the rank correlation between estimated and true edges estimated using binary nodes (panels (c) and (d)). The graphical lasso algorithm experiences serious violations to its multivariate Gaussian assumption, leading to poor performance. The Ising model suffers from a substantial loss of information due to dichotomization of the Gaussian variables.

## 8 Real data analysis

We further compare the four algorithms considered in Section 7.3 using the yeast eQTL data set studied in Brem and Kruglyak (2005), Chen et al. (2011) and Daye et al. (2012). The data consists of gene expression levels and DNA markers measured on yeast segregants. Genes with missing values were removed, and representative markers were selected as described in Chen et al. (2011), leaving  $n = 112$  observations with 5428 gene expression measurements and 585 markers. The gene expression levels are continuous, and we model them as Gaussian; some values of markers are fractional due to imputation (Chen et al., 2011), and we dichotomize them by 0.5 to model

them as binary. In order to obtain network estimates that can be easily displayed, we limited our analysis to the 50 genes and 50 markers with the highest marginal variances. We applied the four algorithms described in Section 7.3. For the sake of comparison, the tuning parameter for each method was chosen to yield around 60 estimated edges.

The four estimated graphs are shown in Figure 3. There are some qualitative differences among the graphs. The estimated marker-marker edges are almost the same across the four estimated graphs, but the gene-gene and gene-marker edges are quite different. In particular, many fewer gene-marker edges are estimated using the graphical lasso algorithm, as compared to the other three algorithms. The reverse holds for the gene-gene edges. Two genes, YPR104C and YCR045C, are connected to the same marker in all but the estimated network from the mixed graphical model neighbourhood selection approach. The gene YJR138W is connected with six markers in the graph resulting from neighbourhood selection in the mixed graphical model, and four in the graph from neighbourhood selection in the Gaussian graphical model. However, this gene is not connected with any markers in the other two graphs.

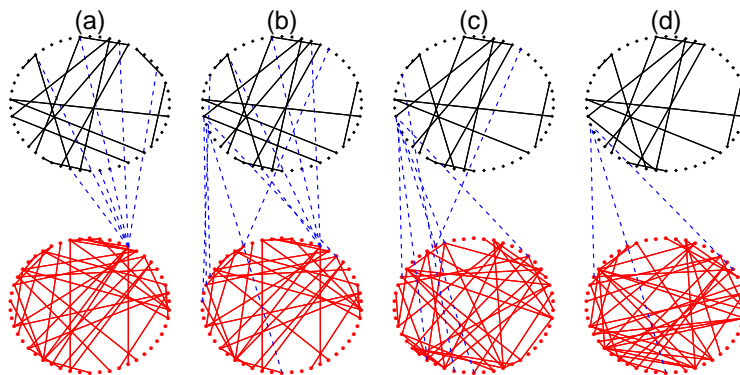


Figure 3: Estimated graphs from four algorithms. 50 genes are shown in red, and 50 markers are shown in black. The four panels display estimated networks from (a) the proposed approach for neighbourhood selection in the mixed graphical model; (b) neighbourhood selection in the Gaussian graphical model; (c) neighbourhood selection in the Ising model, after dichotomizing the Gaussian variables; and (d) graphical lasso applied to the correlation matrix.

## 9 Discussion

More work needs to be done in order to carry the mixed graphical model forward. Here we briefly discuss some possible directions for future work.

In Section 3 we saw that a stringent set of restrictions is required for compatibility or strong compatibility of the node-conditional distributions given in (5)–(8). These restrictions limit the theoretical flexibility of the conditionally-specified mixed graphical model, especially when modeling unbounded variables. It is possible that by truncating unbounded variables, we may be able to circumvent some of these restrictions.

The proposed model (2) assumes pairwise interactions in the form of  $x_s x_t$ , which can be seen as a second-order approximation of the true edge potentials in (1). We can relax the assumption,



for instance, by fitting non-linear edge potentials using non-parametric penalized regressions, as in Voorman et al. (2013).

In future work, rather than taking a neighbourhood selection approach as in (12), we could estimate parameters in the mixed graphical model using a penalized pseudolikelihood approach, as in Höfling and Tibshirani (2009), Peng et al. (2009), and Lee and Hastie (2012). The resulting estimator may have improved efficiency or better empirical performance.

## Acknowledgement

The authors acknowledge funding from the following sources: National Science Foundation grants to D.W. and A.S., National Institutes of Health grants to D.W. and A.S., and a Sloan Foundation Fellowship to D.W. We thank Z. John Daye for providing the data examined in Section 8, and for helpful responses to our inquiries.

## References

- Allen, G. I. and Z. Liu (2012). A log-linear graphical model for inferring genetic networks from high-throughput sequencing data. In *IEEE International Conference on Bioinformatics and Biomedicine*, pp. 1–6. IEEE.
- Arnold, B. C., E. Castillo, and J. M. Sarabia (1999). *Conditional specification of statistical models*. Springer.
- Besag, J. (1974). Spatial interaction and the statistical analysis of lattice systems. *Journal of the Royal Statistical Society, Series B*, 192–236.
- Brem, R. B. and L. Kruglyak (2005). The landscape of genetic complexity across 5,700 gene expression traits in yeast. *Proceedings of the National Academy of Sciences of the United States of America* 102(5), 1572–1577.
- Bunea, F. (2008). Honest variable selection in linear and logistic regression models via  $\ell_1$  and  $\ell_1 + \ell_2$  penalization. *Electronic Journal of Statistics* 2, 1153–1194.
- Chen, J., J. Xie, and H. Li (2011). A penalized likelihood approach for bivariate conditional normal models for dynamic co-expression analysis. *Biometrics* 67(1), 299–308.
- Cheng, J., E. Levina, and J. Zhu (2013). High-dimensional mixed graphical models. *arXiv preprint arXiv:1304.2810*.
- Chernoff, H. (1952). A measure of asymptotic efficiency for tests of a hypothesis based on the sum of observations. *The Annals of Mathematical Statistics* 23(4), 493–507.
- Dai, B., S. Ding, and G. Wahba (2012). Multivariate Bernoulli distribution. *arXiv preprint arXiv:1206.1874*.
- Daye, Z. J., J. Chen, and H. Li (2012). High-dimensional heteroscedastic regression with an application to eQTL data analysis. *Biometrics* 68(1), 316–326.

- Fan, J. and R. Li (2004). New estimation and model selection procedures for semiparametric modeling in longitudinal data analysis. *Journal of the American Statistical Association* 99(467), 710–723.
- Fellinghauer, B., P. Bühlmann, M. Ryffel, M. Von Rhein, and J. D. Reinhardt (2013). Stable graphical model estimation with random forests for discrete, continuous, and mixed variables. *Computational Statistics & Data Analysis* 64, 132–142.
- Finegold, M. and M. Drton (2011). Robust graphical modeling of gene networks using classical and alternative t-distributions. *The Annals of Applied Statistics* 5(2A), 1057–1080.
- Friedman, J., T. Hastie, and R. Tibshirani (2008). Sparse inverse covariance estimation with the graphical lasso. *Biostatistics* 9(3), 432–441.
- Friedman, J., T. Hastie, and R. Tibshirani (2010). Regularization paths for generalized linear models via coordinate descent. *Journal of statistical software* 33(1), 1.
- Höfling, H. and R. Tibshirani (2009). Estimation of sparse binary pairwise Markov networks using pseudo-likelihoods. *The Journal of Machine Learning Research* 10, 883–906.
- Jalali, A., P. D. Ravikumar, V. Vasuki, and S. Sanghavi (2011). On learning discrete graphical models using group-sparse regularization. In *International Conference on Artificial Intelligence and Statistics*, pp. 378–387.
- Lauritzen, S. (1996). *Graphical models*, Volume 17. Oxford University Press, USA.
- Lee, J. and T. Hastie (2012). Learning mixed graphical models. *arXiv preprint arXiv:1205.5012*.
- Lee, S., V. Ganapathi, and D. Koller (2006). Efficient structure learning of Markov networks using  $\ell_1$ -regularization. In *Advances in Neural Information Processing Systems*, pp. 817–824.
- Liu, H., J. Lafferty, and L. Wasserman (2009). The nonparanormal: Semiparametric estimation of high dimensional undirected graphs. *The Journal of Machine Learning Research* 10, 2295–2328.
- Meinshausen, N. and P. Bühlmann (2006). High-dimensional graphs and variable selection with the lasso. *The Annals of Statistics* 34(3), 1436–1462.
- Miyamura, M. and Y. Kano (2006). Robust Gaussian graphical modeling. *Journal of multivariate analysis* 97(7), 1525–1550.
- Peng, J., P. Wang, N. Zhou, and J. Zhu (2009). Partial correlation estimation by joint sparse regression models. *Journal of the American Statistical Association* 104(486), 735–746.
- Ravikumar, P. and J. Lafferty (2004). Variational chernoff bounds for graphical models. In *Proceedings of the 20th conference on Uncertainty in artificial intelligence*, pp. 462–469. AUAI Press.
- Ravikumar, P., M. Wainwright, and J. Lafferty (2010). High-dimensional Ising model selection using  $\ell_1$ -regularized logistic regression. *The Annals of Statistics* 38(3), 1287–1319.

- Ravikumar, P., M. J. Wainwright, G. Raskutti, and B. Yu (2011). High-dimensional covariance estimation by minimizing  $\ell_1$ -penalized log-determinant divergence. *Electronic Journal of Statistics* 5, 935–980.
- Rothman, A. J., P. J. Bickel, E. Levina, and J. Zhu (2008). Sparse permutation invariant covariance estimation. *Electronic Journal of Statistics* 2, 494–515.
- Sun, H. and H. Li (2012). Robust Gaussian graphical modeling via  $\ell_1$  penalization. *Biometrics* 68(4), 1197–1206.
- van de Geer, S., P. Bühlmann, and Y. Ritov (2013). On asymptotically optimal confidence regions and tests for high-dimensional models. *arXiv preprint arXiv:1303.0518*.
- Van de Geer, S. A. (2008). High-dimensional generalized linear models and the lasso. *The Annals of Statistics* 36(2), 614–645.
- Voorman, A., A. Shojaie, and D. Witten (2013). Graph estimation with joint additive models. *Biometrika*.
- Wainwright, M. (2009). Sharp thresholds for high-dimensional and noisy sparsity recovery using  $\ell_1$ -constrained quadratic programming (lasso). *Information Theory, IEEE Transactions on* 55(5), 2183–2202.
- Wainwright, M. J. and M. I. Jordan (2008). Graphical models, exponential families, and variational inference. *Foundations and Trends in Machine Learning* 1(1-2), 1–305.
- Wainwright, M. J., J. D. Lafferty, and P. K. Ravikumar (2006). High-dimensional graphical model selection using  $\ell_1$ -regularized logistic regression. In *Advances in neural information processing systems*, pp. 1465–1472.
- Wang, Y. J. and E. H. Ip (2008). Conditionally specified continuous distributions. *Biometrika* 95(3), 735–746.
- Xue, L. and H. Zou (2012). Regularized rank-based estimation of high-dimensional nonparanormal graphical models. *The Annals of Statistics* 40(5), 2541–2571.
- Yang, E., P. Ravikumar, G. Allen, and Z. Liu (2012). Graphical models via generalized linear models. In *Advances in Neural Information Processing Systems* 25, pp. 1367–1375.
- Yang, E., P. Ravikumar, G. I. Allen, and Z. Liu (2013). On graphical models via univariate exponential family distributions. *arXiv preprint arXiv:1301.4183*.
- Yuan, M. and Y. Lin (2007). Model selection and estimation in the Gaussian graphical model. *Biometrika* 94(1), 19–35.

# A Supplementary material: Selection and Estimation for Mixed Graphical Models

## A.1 A Proof for Proposition 1

*Proof.* First of all, it is easy to see that if  $\theta_{st} = \theta_{ts}$ , then any function  $g$  such that

$$g(x) \propto \exp \left\{ \sum_{s=1}^p f_s(x_s) + \frac{1}{2} \sum_{s=1}^p \sum_{t \neq s} \theta_{ts} x_s x_t \right\} \quad (27)$$

is capable of generating the conditional densities (4) as long as the function  $g$  is integrable with respect to  $x_s$  for  $s = 1, \dots, p$ . The function  $g$  can be decomposed as

$$g(x) \propto \exp \left\{ f_s(x_s) + \frac{1}{2} \sum_{t:t \neq s} \theta_{ts} x_s x_t \right\} \exp \left\{ \sum_{t \neq s} f_t(x_t) + \frac{1}{2} \sum_{t:t \neq s, j:j \neq s, j \neq t} \theta_{tj} x_j x_t \right\},$$

so the integrability of the conditional density  $p(x_s | x_{-s})$  (4) guarantees the integrability of  $g$  with respect to  $x_s$ . Therefore, the conditional densities of the form (4) are compatible if  $\theta_{ts} = \theta_{st}$ .

We now prove that any function  $h$  that is capable of generating the conditional density (4) is in the form of (27). The following proof is essentially the same as that in Besag (1974). Suppose  $h$  is a function that is capable of generating the conditional densities in (4). Define  $P(x) = \log\{h(x)/h(0)\}$ , where 0 can be replaced by any interior point in the sample space.

By definition,  $P(0) = \log\{h(0)/h(0)\} = 0$ . Therefore,  $P(\cdot)$  can be written in the general form

$$P(x) = \sum_{s=1}^p x_s G_s(x_s) + \frac{1}{2} \sum_{t \neq s} G_{ts}(x_t, x_s) x_t x_s + \frac{1}{6} \sum_{t \neq s, t \neq j, j \neq s} G_{tsj}(x_t, x_s, x_j) x_t x_s x_j + \dots \quad (28)$$

In (28), we write the function  $P$  as the sum of interactions of different orders. Note that the factor of  $1/2$  in (28) is due to the fact that  $G_{st}(x_s, x_t) = G_{ts}(x_t, x_s)$ ; similar factors apply for higher-order interactions. Recalling that we assume  $h$  is capable of generating the conditional density  $p(x_s | x_{-s})$ , from Definition 1 we know that

$$P(x) - P(x_s^0) = \log \left\{ \frac{h(x) / \int h(x) dx}{h(x_s^0) / \int h(x) dx} \right\} = \log \left\{ \frac{p(x_s | x_{-s})}{p(0 | x_{-s})} \right\},$$

where  $x_s^0 = (x_1, \dots, x_{s-1}, 0, x_{s+1}, \dots, x_p)^T$  and  $p(x_s | x_{-s})$  is the conditional density in (4). It follows that

$$\log \left\{ \frac{p(x_s | x_{-s})}{p(0 | x_{-s})} \right\} = P(x) - P(x_s^0) = x_s \left( G_s(x_s) + \sum_{t:t \neq s} x_t G_{ts}(x_t, x_s) + \dots \right). \quad (29)$$

Letting  $x_t = 0$  for  $t \neq s$  in (29) and using the form of the conditional densities in (4), we have

$$x_s G_s(x_s) = f_s(x_s) - f_s(0). \quad (30)$$

Here we set  $f_s(0) = 0$  since  $f_s(0)$  is a constant. For the second-order interaction  $G_{ts}$ , we let  $x_j = 0$  for  $j \neq t, j \neq s$  in (29):

$$x_s G_s(x_s) + x_s x_t G_{ts}(x_t, x_s) = \theta_{st} x_t x_s + f_s(x_s).$$

Similarly, applying the previous argument on  $P(x) - P(x_t^0)$ , we have

$$x_t G_t(x_t) + x_s x_t G_{st}(x_s, x_t) = \theta_{ts} x_t x_s + f_t(x_t).$$

Therefore, if  $\theta_{st} = \theta_{ts}$ , then by (30),

$$G_{st}(x_s, x_t) = G_{ts}(x_t, x_s) = \theta_{st}.$$

It is easy to show that, by setting  $x_k = 0$  ( $k \neq s, k \neq t, k \neq j$ ) in (29), the third-order interactions in  $P(x)$  are zero. Similarly, we can show that fourth-and-higher-order interactions are zero. Hence, we arrive at the following formula for  $P$ :

$$P(x) = \sum_{s=1}^p f_s(x_s) + \frac{1}{2} \sum_{s=1}^p \sum_{t \neq s}^p \theta_{ts} x_s x_t.$$

Furthermore,  $P(x) = \log\{h(x)/h(0)\}$ , so the function  $h$  takes the form

$$h(x) \propto \exp\{P(x)\} = \exp\left\{\sum_{s=1}^p f_s(x_s) + \frac{1}{2} \sum_{s=1}^p \sum_{t \neq s}^p \theta_{ts} x_s x_t\right\},$$

which is the same as (27). □

## A.2 A Proof for Lemma 1

*Proof.* It is easy to verify using basic calculus that the conditional densities are integrable given the restrictions in Lemma 1. Therefore, these restrictions are sufficient for compatibility.

We now show that the restrictions in Lemma 1 are necessary, by investigating each of the distributions in (5)–(8). Recall that we have limited our discussion in the case where the joint distribution is non-degenerate.

Suppose that  $x_s \mid x_{-s}$  is exponential, as in (8). By definition of the exponential distribution, it must be that  $\eta = \alpha_{1s} + \sum_{t \neq s} \theta_{ts} x_t < 0$ . This leads to the following restrictions on  $\theta_{ts}$ : 1) When  $x_t$  is Poisson or exponential, it must be that  $\theta_{ts} \leq 0$ . 2) When  $x_t$  is Gaussian, then it must be that  $\theta_{ts} = 0$ . 3) Let  $I$  denote the indices of the binary variables. Then it must be that  $\sum_{t \in I} |\theta_{ts}| < -\alpha_{1s}$ .

Suppose that  $x_s \mid x_{-s}$  is Gaussian, as in (5). Then  $\alpha_{2s}$  has to be negative for the conditional density to be well-defined.

Suppose that  $x_s \mid x_{-s}$  is binary (6) or Poisson (7). We can see that there are no restrictions on  $\eta$ , and thus no restrictions on  $\theta_{ts}$  or  $\alpha_{1s}$ .

Hence, the conditions in Lemma 1 are necessary for the conditional densities in (5)–(8) to be compatible. □

### A.3 A Proof for Lemma 2

*Proof.* We first prove the necessity of the conditions in Table 1. Recall from Definition 1 that in order for strong compatibility to hold, compatibility must hold, and the function  $g$  in (9) must be a density. The conditions for compatibility were given in Lemma 1. We now derive the necessary conditions for  $g$  to be a density.

For Gaussian nodes that are indexed by  $J$ , recall that  $\Theta_{JJ}$  is defined as in (11). We know from the property of the multivariate Gaussian distribution that  $\Theta_{JJ}$  must be negative definite if the joint density exists and is non-degenerate.

Let  $x_1$  be a Poisson node, and  $x_2$  an exponential node. Consider the ratio

$$G(x_1, x_2) = \frac{g(x_1, x_2, 0, \dots, 0)}{g(0, 0, 0, \dots, 0)} = \exp\{-\log(x_1!) + \alpha_{11}x_1 + \theta_{12}x_1x_2 + \alpha_{12}x_2\},$$

where  $g$  is the function in (10). It is not hard to see that integrability of  $G(x_1, x_2)$  is a necessary condition for integrability of the joint density. Summing over  $x_1$  yields

$$\sum_{i=0}^{\infty} G(i, x_2) = \exp\{\alpha_{12}x_2 + \exp(\alpha_{11} + \theta_{12}x_2)\}.$$

Therefore, in order for  $\sum_{i=0}^{\infty} G(i, x_2)$  to be integrable with respect to the exponential node  $x_2$ , it must be the case that  $\theta_{12} = \theta_{21} \leq 0$ . Following a similar argument, the edge potential  $\theta_{12} = \theta_{21}$  has to be non-positive when  $x_2$  is Poisson, and zero when  $x_2$  is Gaussian.

A similar argument to the one just described can be applied to the exponential nodes. Such an argument reveals that the conditions on the edge potentials of the exponential nodes that are necessary in order for  $g$  to be a density are those stated in Lemma 1.

For binary nodes, no restrictions on the edge potentials are necessary in order for  $g$  to be a density.

Therefore, the conditions listed in Table 1 are necessary for the conditional densities in (5)–(8) to be strongly compatible.

We now show that the conditions listed in Table 1 are sufficient for the conditional densities to be strongly compatible. First, we restrict the discussion by conditioning on the binary nodes, since integrating binary variables yields a mixture of finite components. Second, the Gaussian nodes are isolated from the Poisson and exponential nodes, as the edge potentials between Gaussian and the other two types of nodes are zero. Third, the distribution of Gaussian nodes is integrable as  $\Theta_{JJ}$  is negative definite, where  $\Theta_{JJ}$  is as in (11). Now we consider just the Poisson and exponential nodes. For these,

$$\exp\left\{\sum_{s=1}^p f_s(x_s) + \frac{1}{2} \sum_{s=1}^p \sum_{t \neq s}^p \theta_{st} x_s x_t\right\} \leq \exp\left\{\sum_{s=1}^p f_s(x_s)\right\}$$

since  $\theta_{st} x_s x_t \leq 0$ . So the joint density is dominated by the density of a model with no interactions, which is integrable given that  $\alpha_{1s}$  for an exponential node  $x_s$  is non-positive. Hence, the conditions listed in Table 1 are also sufficient for the conditional densities in (5)–(8) to be strongly compatible.  $\square$

## A.4 A Proof for Theorem 1

*Proof.* Our proof is similar to that of Theorem 2 in Yang et al. (2013), and is based on the primal-dual witness method (Wainwright, 2009). The primal-dual witness method studies the property of  $\ell_1$ -penalized estimators by investigating the sub-gradient condition of an oracle estimator. We assume that readers are familiar with the primal-dual witness method; for reference, see Ravikumar et al. (2011) and Yang et al. (2013). Without loss of generality, we assume  $s = p$  to avoid cumbersome notation. For other values of  $s$ , a similar proof holds with more complicated notation. Below we denote  $\Theta_p$  as  $\theta$  and  $\ell_p$  as  $\ell$  for simplicity.

The sub-gradient condition for the optimization problem (12) with respect to  $(\theta^\top, \alpha_{1p}^\top)^\top$  is

$$-\nabla\ell(\hat{\theta}, \hat{\alpha}_{1p}; X) + \lambda_n \hat{Z} = 0; \quad \hat{Z}_t = \text{sgn}(\hat{\theta}_t) \quad t < p; \quad \hat{Z}_p = 0, \quad (31)$$

where

$$\text{sgn}(x) = \begin{cases} x/|x| & x \neq 0, \\ \gamma \in [-1, 1] & x = 0. \end{cases}$$

We construct the oracle estimator  $(\hat{\theta}_N^\top, \hat{\theta}_\Delta^\top, \hat{\alpha}_{1p}^\top)^\top$  as follows: first, let  $\hat{\theta}_\Delta = 0$ ; second, obtain  $\hat{\theta}_N, \hat{\alpha}_{1p}$  by solving (12) with an additional restriction that  $\hat{\theta}_\Delta = 0$ ; third, set  $\hat{Z}_t = \text{sgn}(\hat{\theta}_t)$  for  $t \in N$  and  $\hat{Z}_p = 0$ ; last, estimate  $\hat{Z}_\Delta$  from (31) by plugging in  $\hat{\theta}, \hat{\alpha}_{1p}$  and  $\hat{Z}_{\Delta^c}$ . To complete the proof, we verify that  $(\hat{\theta}_N^\top, \hat{\theta}_\Delta^\top, \hat{\alpha}_{1p}^\top)^\top$  and  $\hat{Z} = (\hat{Z}_N^\top, \hat{Z}_\Delta^\top, 0)^\top$  is a primal-dual pair of (12) and recovers the true neighbourhood exactly.

Applying the mean value theorem on each element of  $\nabla\ell(\hat{\theta}, \hat{\alpha}_{1p}; X)$  in the subgradient condition (31) gives

$$Q^* \begin{pmatrix} \hat{\theta} - \theta^* \\ \hat{\alpha}_{1p} - \alpha_{1p}^* \end{pmatrix} = -\lambda_n \hat{Z} + W^n + R^n, \quad (32)$$

where  $W^n = \nabla\ell(\theta^*, \alpha_{1p}^*; X)$  is the sample score function evaluated at the true parameter  $(\theta^{*\top}, \alpha_{1p}^{*\top})^\top$ . In (32),  $R^n$  is the residual term from the mean value theorem, whose  $k$ th term is given by

$$R_k^n = [\nabla^2\ell(\bar{\theta}^k, \bar{\alpha}_{1p}^k; X) - \nabla^2\ell(\theta^*, \alpha_{1p}^*; X)]_k^\top \begin{pmatrix} \hat{\theta} - \theta^* \\ \hat{\alpha}_{1p} - \alpha_{1p}^* \end{pmatrix}, \quad (33)$$

where  $(\bar{\theta}^\top, \bar{\alpha})^\top$  denotes an intermediate point between  $(\theta^{*\top}, \alpha_{1p}^{*\top})^\top$  and  $(\hat{\theta}^\top, \hat{\alpha}_{1p}^\top)^\top$ , and  $[\cdot]_k^\top$  denotes the  $k$ th row of a matrix.

By construction,  $\hat{\theta}_\Delta = 0$ . Thus, (32) can be rearranged as

$$\lambda_n \hat{Z}_\Delta = (W_\Delta^n + R_\Delta^n) - Q_{\Delta\Delta^c}^* (Q_{\Delta^c\Delta^c}^*)^{-1} (W_{\Delta^c}^n + R_{\Delta^c}^n - \lambda_n \hat{Z}_{\Delta^c}). \quad (34)$$

Therefore, the estimator  $\hat{Z}_\Delta$  that we get from plugging in  $\hat{\theta}, \hat{\alpha}_{1p}$  and  $\hat{Z}_{\Delta^c}$  must satisfy (34). To complete the proof, we need to verify strict dual feasibility,

$$\|\hat{Z}_\Delta\|_\infty < 1, \quad (35)$$

and sign consistency,

$$\text{sgn}(\hat{\theta}_t) = \text{sgn}(\theta_t^*) \quad \text{for any } t \in N. \quad (36)$$

In (32),  $\max_{l \in \Delta} \|Q_{l\Delta^c}^* (Q_{\Delta^c\Delta^c}^*)^{-1}\|_1 \leq 1 - a$  by Assumption 1. The following lemmas characterize useful concentration inequalities regarding  $W^n$ ,  $R^n$ , and  $\hat{\theta}_N - \theta_N^*$ . Proofs of Lemmas A4 and A5 are given in Sections A.5 and A.6, respectively.

**Lemma 4.** Suppose that

$$\frac{8(2-a)}{a} \{\delta_2 \kappa_2 \log(2p)/n\}^{1/2} \leq \lambda_n \leq \frac{2(2-a)}{a} \delta_2 \kappa_2 M,$$

where  $\delta_2$  is defined in Proposition 3, and  $a$  and  $\kappa_2$  are defined in Assumptions 1 and 3, respectively. Then,

$$\text{pr} \left( \|W^n\|_\infty > \frac{a\lambda_n}{8-4a} \mid \xi_2, \xi_1 \right) \leq \exp(-c_3 \delta_3 n),$$

where  $\delta_3 = 1/(\kappa_2 \delta_2)$  and  $c_3$  is some positive constant.

**Lemma 5.** Suppose that  $\xi_1$  and  $\|W^n\|_\infty \leq a\lambda_n/(8-4a)$  hold and

$$\lambda_n \leq \min \left\{ \frac{a\Lambda_1^2(d+1)^{-1}}{288(2-a)\kappa_2\Lambda_2}, \frac{\Lambda_1^2(d+1)^{-1}}{12\Lambda_2\kappa_3\delta_1 \log p} \right\},$$

where  $\delta_1$  is defined in Proposition 2, and  $a$  and  $\kappa_3$  are defined in Assumptions 1 and 3, respectively. Then with probability 1,

$$\|\hat{\theta}_N - \theta_N^*\|_2 < \frac{10}{\Lambda_1} (d+1)^{1/2} \lambda_n, \quad \|R^n\|_\infty \leq \frac{a\lambda_n}{8-4a}.$$

We now continue with the proof of Theorem 1. Given Condition 2, the conditions regarding  $\lambda_n$  are met for Lemmas A4 and A5.

We now assume that  $\xi_1, \xi_2$  and the event  $\|W^n\|_\infty \leq a\lambda_n/(8-4a)$  are true so that the conditions for the two lemmas are satisfied. We show that these events happen with high probability at the end of the proof.

First, applying Lemma A5 and Assumption 1 to (34) yields

$$\begin{aligned} \|\hat{Z}_\Delta\|_\infty &\leq \max_{l \in \Delta} \|Q_{l\Delta^c}^* (Q_{\Delta^c\Delta^c}^*)^{-1}\|_1 \left( \|W_{\Delta^c}^n\|_\infty + \|R_{\Delta^c}^n\|_\infty + \lambda_n \|\hat{Z}_{\Delta^c}\|_\infty \right) / \lambda_n + \\ &\quad (\|W_\Delta^n\|_\infty + \|R_\Delta^n\|_\infty) / \lambda_n \\ &\leq (1-a) + (2-a) \left\{ \frac{a}{4(2-a)} + \frac{a}{4(2-a)} \right\} < 1. \end{aligned} \tag{37}$$

Next, applying Lemma A5 and a norm inequality to  $\|\hat{\theta}_N - \theta_N^*\|_\infty$  gives

$$\|\hat{\theta}_N - \theta_N^*\|_\infty \leq \|\hat{\theta}_N - \theta_N^*\|_2 < \frac{10}{\Lambda_1} (d+1)^{1/2} \lambda_n \leq \min_t \{\theta_t\}, \tag{38}$$

since  $\min_t \{\theta_t\} \geq 10(d+1)^{1/2} \lambda_n / \Lambda_1$  by Condition 1. The strict inequality (38) ensures that the sign of the estimator is consistent with the sign of the true value for all edges.

(37) and (38) are sufficient to establish the result (i.e.  $\hat{N} = N$ ). Let  $A$  be the event  $\|W^n\|_\infty \leq a\lambda_n/(8-4a)$ . Recall that we have assumed events  $A, \xi_1$ , and  $\xi_2$  to be true in order to prove (37) and (38). We now show that  $A \cap \xi_1 \cap \xi_2$  happens with high probability.

Using the fact that

$$\text{pr}\{(A \cap \xi_1 \cap \xi_2)^c\} \leq \text{pr}(A^c \mid \xi_1 \cap \xi_2) + \text{pr}\{(\xi_1 \cap \xi_2)^c\} \leq \text{pr}(A^c \mid \xi_1, \xi_2) + \text{pr}(\xi_1^c) + \text{pr}(\xi_2^c),$$



we know the probability of  $A \cap \xi_1 \cap \xi_2$  satisfies

$$\text{pr} \left\{ \left( \|W^n\|_\infty \leq \frac{a}{2-a} \frac{\lambda_n}{4} \right) \cap \xi_2 \cap \xi_1 \right\} \geq 1 - c_1 p^{-\delta_1+2} - \exp(-c_2 \delta_2^2 n) - \exp(-c_3 \delta_3 n),$$

where  $c_1$ ,  $c_2$ , and  $c_3$  are constants from Proposition 2, Proposition 3, and Lemma A4. This completes the proof.  $\square$

## A.5 A Proof for Lemma A4

*Proof.* Recall that  $\eta^{(i)} = \alpha_{1p} + \sum_{t < p} \theta_t x_t^{(i)}$  and that we have assumed that  $\alpha_{kp}$  is known for  $k \geq 2$ . We can rewrite the conditional density (4) as

$$p(x_p \mid x_{-p}) \propto \exp\{\eta x_p - D(\eta)\}.$$

For any  $t < p$ ,

$$W_t^n = \frac{\partial \ell}{\partial \theta_t} = \sum_{i=1}^n \frac{\partial \ell}{\partial \eta^{(i)}} \frac{\partial \eta^{(i)}}{\partial \theta_t} = \frac{1}{n} \sum_{i=1}^n \{x_p^{(i)} - D'(\eta^{(i)})\} x_t^{(i)}. \quad (39)$$

Recall that  $M$  is a large constant introduced in Assumption 3. Suppose that  $M$  is so large that  $|\alpha_{1p}^*| + \sum_{k < p} |\theta_k^*| < M/2$ . For every  $v$  such that  $0 < v < M/2$ ,

$$\begin{aligned} E \left[ \exp \left\{ v x_t^{(i)} \left( x_p^{(i)} - D'(\eta^{(i)}) \right) \right\} \mid X_{-p} \right] &= E \left[ \exp \left\{ v x_t^{(i)} x_p^{(i)} \right\} \mid X_{-p} \right] \exp \left( -v x_t^{(i)} D'(\eta^{(i)}) \right) \\ &= \exp \left( D(\eta^{(i)} + v x_t^{(i)}) - D(\eta^{(i)}) \right) \exp \left( -v x_t^{(i)} D'(\eta^{(i)}) \right) \\ &= \exp \left( v x_t^{(i)} D'(\eta^{(i)}) + (v x_t^{(i)})^2 \frac{D''(\tilde{\eta})}{2} \right) \exp \left( -v x_t^{(i)} D'(\eta^{(i)}) \right) \\ &= \exp \left\{ (v x_t^{(i)})^2 \frac{D''(\tilde{\eta})}{2} \right\} \quad (\tilde{\eta} \in [\eta^{(i)}, \eta^{(i)} + v x_t^{(i)}]), \end{aligned} \quad (40)$$

where the second equality was derived using the properties of the moment generating function of the exponential family, and the third equality follows from a second-order Taylor expansion. Since  $\tilde{\eta} \in [\eta^{(i)}, \eta^{(i)} + v x_t^{(i)}]$ , the event  $\xi_1$  implies that

$$|\tilde{\eta}| \leq |\alpha_{1p}^*| + \sum_{k < p} |x_k^{(i)} \theta_k^*| + |v x_t^{(i)}| \leq |\alpha_{1p}^*| + \left( \sum_{k < p} |\theta_k^*| + |v| \right) \max_{t,i} \{|x_t^{(i)}|\} \leq M \delta_1 \log p. \quad (41)$$

Therefore, the condition of Assumption 3 is satisfied, and thus  $|D''(\tilde{\eta})| \leq \kappa_2$ . Recalling that  $\{x^{(i)}\}_{i=1}^n$  are independent samples, it follows that

$$\begin{aligned} E \left[ \exp\{v n W_t^n\} \mid \xi_2, \xi_1 \right] &= E \left[ E \left\{ \exp(v n W_t^n) \mid X_{-p}, \xi_2, \xi_1 \right\} \mid \xi_2, \xi_1 \right] \\ &\leq E \left[ \exp \left\{ v^2 \frac{\kappa_2}{2} \sum_{i=1}^n (x_t^{(i)})^2 \right\} \mid \xi_2, \xi_1 \right] \\ &\leq \exp\{n v^2 \kappa_2 \delta_2 / 2\}, \end{aligned} \quad (42)$$

where we use the event  $\xi_2$  in the last inequality. Similarly,

$$E[\exp\{-nvW_t^n\} \mid \xi_2, \xi_1] \leq \exp\{nv^2\kappa_2\delta_2/2\}. \quad (43)$$

Furthermore, one can see from a similar argument as in (39) and (40) that

$$\begin{aligned} E[\exp\{nvW_p^n\} \mid \xi_1] &= E\left[\exp\left\{vn\frac{\partial\ell}{\partial\alpha_{1p}}\right\} \mid \xi_1\right] \\ &= \prod_{i=1}^n E\left[\exp\{v(x_p^{(i)} - D'(\eta^{(i)}))\} \mid \xi_1\right] \leq \exp\{n\kappa_2v^2/2\}. \end{aligned}$$

We focus on the discussion of (42) since  $\delta_2 \geq 1$ . For some  $\delta$  to be specified, we let  $v = \delta/(\kappa_2\delta_2)$  and apply the Chernoff bound (Chernoff, 1952; Ravikumar and Lafferty, 2004) with (42) and (43) to get

$$\text{pr}(|W_t^n| > \delta \mid \xi_2, \xi_1) \leq \frac{E[\exp(vnW_t^n) \mid \xi_2, \xi_1]}{\exp(vn\delta)} + \frac{E[\exp(-vnW_t^n) \mid \xi_2, \xi_1]}{\exp(vn\delta)} \leq 2 \exp\left(-n\frac{\delta^2}{2\kappa_2\delta_2}\right).$$

Letting  $\delta = a\lambda_n/(8 - 4a)$  and using the Bonferroni inequality, we get

$$\begin{aligned} \text{pr}\left(\|W^n\|_\infty > \frac{a}{2-a}\frac{\lambda_n}{4} \mid \xi_2, \xi_1\right) &\leq 2 \exp\left\{-n\frac{a^2\lambda_n^2}{32(2-a)^2\kappa_2\delta_2} + \log(p)\right\} \\ &\leq \exp\left\{-\frac{a^2\lambda_n^2}{64(2-a)^2\kappa_2\delta_2}n\right\} = \exp(-c_3\delta_3n), \end{aligned} \quad (44)$$

where  $\delta_3 = 1/(\kappa_2\delta_2)$  and  $c_3 = a^2\lambda_n^2/\{64(2-a)^2\}$ . In (44), we made use of the assumption that  $\lambda_n \geq 8(2-a)\{\kappa_2\delta_2 \log(2p)/n\}^{1/2}/a$ , and we also require that  $\lambda_n \leq 2(2-a)\kappa_2\delta_2 M/a$  since  $v = a\lambda_n/[(8-4a)\kappa_2\delta_2] \leq M/2$ .  $\square$

## A.6 A Proof for Lemma A5

*Proof.* We first prove that  $\|\hat{\theta}_N - \theta_N^*\|_2 < \frac{10}{\Lambda_1}(d+1)^{1/2}\lambda_n$ .

Following the method in Fan and Li (2004) and Ravikumar et al. (2010), we construct a function  $F(u)$  as

$$F(u) = -\ell(\theta^* + u_{-p}, \alpha_{1p}^* + u_p; X) + \ell(\theta^*, \alpha_{1p}^*; X) + \lambda_n\|\theta^* + u_{-p}\|_1 - \lambda_n\|\theta^*\|_1, \quad (45)$$

where  $u$  is a  $p$ -dimensional vector and  $u_\Delta = 0$ .  $F(u)$  has some nice properties: (i)  $F(0) = 0$  by definition; (ii)  $F(u)$  is convex in  $u$  given the form of (4); and (iii) by the construction of the oracle estimator  $\hat{\theta}$ ,  $F(u)$  is minimized by  $\hat{u}$  with  $\hat{u}_{-p} = \hat{\theta} - \theta^*$  and  $\hat{u}_p = \hat{\alpha}_{1p} - \alpha_{1p}^*$ .

We claim that if there exists a constant  $B$  such that  $F(u) > 0$  for any  $u$  such that  $\|u\|_2 = B$  and  $u_\Delta = 0$ , then  $\|\hat{u}\|_2 \leq B$ . To show this, suppose that  $\|\hat{u}\|_2 > B$  for such a constant. Let  $t = B/\|\hat{u}\|_2$ . Then,  $t < 1$ , and the convexity of  $F(u)$  gives

$$F(t\hat{u}) \leq (1-t)F(0) + tF(\hat{u}) \leq 0.$$

Thus,  $\|t\hat{u}\|_2 = B$  and  $(t\hat{u})_\Delta = t\hat{u}_\Delta = 0$ , but  $F(t\hat{u}) \leq 0$ , which is a contradiction.

Applying a Taylor expansion to the first term of  $F(u)$  gives

$$\begin{aligned} F(u) &= -\nabla\ell(\theta^*, \alpha_{1p}^*; X)^T u - u^T \nabla^2\ell(\theta^* + vu_{-p}, \alpha_{1p}^* + vu_p; X)u/2 + \lambda_n(\|\theta^* + u_{-p}\|_1 - \|\theta^*\|_1) \\ &= \text{I} + \text{II}/2 + \text{III}, \end{aligned} \tag{46}$$

for some  $v \in [0, 1]$ . Recall that  $u_\Delta = 0$  as defined in (45). The gradient and Hessian are with respect to the vector  $(\theta^T, \alpha_{1p})^T$ .

We now proceed to find a  $B$  such that for  $\|u\|_2 = B$  and  $u_\Delta = 0$ , the function  $F(u)$  is always greater than 0. First, given that  $\|W^n\|_\infty \leq a\lambda_n/(8 - 4a)$  and  $a < 1$  assumed in Assumption 1,

$$|\text{I}| = |(W^n)^T u| \leq \|W^n\|_\infty \|u\|_1 \leq \frac{a}{2-a} \frac{\lambda_n}{4} (d+1)^{1/2} B \leq \frac{\lambda_n}{4} (d+1)^{1/2} B.$$

Next, by the Cauchy-Schwarz inequality,

$$\text{III} \geq -\lambda_n \|u_{-p}\|_1 \geq -\lambda_n d^{1/2} \|u_{-p}\|_2 \geq -\lambda_n (d+1)^{1/2} B.$$

To bound II in (46), we note that

$$-\nabla^2\ell(\theta^* + vu_{-p}, \alpha_{1p}^* + vu_p; X) = \frac{1}{n} \sum_{i=1}^n x_0^{(i)} (x_0^{(i)})^T D''(\eta_r^{(i)}),$$

where  $x_0 = (x_{-p}^T, 1)^T$  as in Assumption 2, and  $\eta_r^{(i)} = \alpha_{1p}^* + vu_p + \sum_{t < p} (\theta_t^* + vu_t) x_t^{(i)}$ . Applying a Taylor expansion on each  $D''(\eta_r^{(i)})$  at  $\eta^{(i)} = \alpha_{1p}^* + \sum_{t < p} \theta_t^* x_t^{(i)}$ , we get

$$\begin{aligned} -\nabla^2\ell(\theta^* + vu_{-p}, \alpha_{1p}^* + vu_p; X) &= \frac{1}{n} \sum_{i=1}^n x_0^{(i)} (x_0^{(i)})^T D''(\eta^{(i)}) + \frac{1}{n} \sum_{i=1}^n x_0^{(i)} (x_0^{(i)})^T D'''(\tilde{\eta}^{(i)}) (vu^T x_0^{(i)}) \\ &= Q^* + \frac{1}{n} \sum_{i=1}^n x_0^{(i)} (x_0^{(i)})^T D'''(\tilde{\eta}^{(i)}) (vu^T x_0^{(i)}), \end{aligned}$$

where  $\tilde{\eta}^{(i)} \in [\eta^{(i)}, \eta_r^{(i)}]$ . Using the argument on  $\tilde{\eta}$  in (41), we can see that  $\tilde{\eta}^{(i)}$  is in the range required for Assumption 3 to hold given  $\xi_1$ . Therefore, applying Assumption 3 we can write

$$\begin{aligned} \text{II} &\geq \min_{u: \|u\|_2=B, u_\Delta=0} \{-u^T \nabla^2\ell(\theta^* + vu_{-p}, \alpha_{1p}^* + vu_p; X)u\} \\ &\geq B^2 \Lambda_{\min}(Q_{\Delta^c \Delta^c}^*) - \max_{v \in [0,1]} \max_{u: \|u\|_2=B, u_\Delta=0} u^T \left\{ \frac{1}{n} \sum_{i=1}^n D'''(\tilde{\eta}^{(i)}) (vu^T x_0^{(i)}) x_0^{(i)} (x_0^{(i)})^T \right\} u \\ &\geq \Lambda_1 B^2 - \max_{u: \|u\|_2=B, u_\Delta=0} \left\{ \max_{i,v \in [0,1]} (vu^T x_0^{(i)}) \max(D'''(\tilde{\eta}^{(i)})) \frac{1}{n} \sum_{i=1}^n (u^T x_0^{(i)})^2 \right\}. \\ &\geq \Lambda_1 B^2 - \kappa_3 \max_{i,u: \|u\|_2=B, u_\Delta=0, v \in [0,1]} (vu^T x_0^{(i)}) \max_{u: \|u\|_2=B, u_\Delta=0} \left\{ \frac{1}{n} \sum_{i=1}^n (u^T x_0^{(i)})^2 \right\} \end{aligned}$$

By inspection, the maximum of  $u^\top x_0^{(i)}$  is non-negative. Thus, the maximum of  $vu^\top x_0^{(i)}$  is achieved at  $v = 1$ . Then, using  $\xi_1$  and Assumption 2,

$$\begin{aligned}\Pi &\geq \Lambda_1 B^2 - \kappa_3 B(d+1)^{1/2} \delta_1 \log(p) B^2 \Lambda_{\max} \left( \frac{1}{n} \sum_{i=1}^n x_0^{(i)} (x_0^{(i)})^\top \right) \\ &\geq \Lambda_1 B^2 - \kappa_3 B^3 (d+1)^{1/2} \delta_1 \log(p) \Lambda_2.\end{aligned}$$

Thus, if the  $B$  we choose satisfies

$$\Lambda_1 - \delta_1 \log(p) B \kappa_3 (d+1)^{1/2} \Lambda_2 \geq \frac{\Lambda_1}{2}, \quad (47)$$

then the lower bound of  $F(u)$  is

$$F(u) \geq -\frac{\lambda_n}{4} (d+1)^{1/2} B + \frac{\Lambda_1}{4} B^2 - \lambda_n (d+1)^{1/2} B.$$

So,  $F(u) > 0$  for any  $B > 5\lambda_n (d+1)^{1/2} / (\Lambda_1)$ . We can hence let

$$B = 6(d+1)^{1/2} \lambda_n / \Lambda_1 \quad (48)$$

to get

$$\|\hat{\theta}_N - \theta_N^*\|_2 \leq \|\hat{u}\|_2 \leq B = \frac{6}{\Lambda_1} (d+1)^{1/2} \lambda_n.$$

And thus,  $\|\hat{\theta}_N - \theta_N^*\|_2 < 10\lambda_n (d+1)^{1/2} / \Lambda_1$ . It is easy to show that (48) satisfies (47) provided that

$$\lambda_n \leq \frac{\Lambda_1^2 (d+1)^{-1}}{12\Lambda_2 \kappa_3 \delta_1 \log p}.$$

To find the bound for  $R^n$  defined in (33), we first recall that  $(\bar{\theta}^\top, \bar{\alpha})^\top$  is an intermediate point between  $(\theta^{*\top}, \alpha_{1p}^*)^\top$  and  $(\hat{\theta}^\top, \hat{\alpha}_{1p})^\top$ . We denote  $\bar{\eta}^{(i)} = \bar{\alpha}_{1p} + \sum_{t < p} \bar{\theta}_t x_t^{(i)}$ , and observe that  $|\bar{\eta}^{(i)}| \leq M\delta_1 \log p$  for  $i = 1, \dots, n$  using the argument of (41), which implies that Assumption 3 is applicable. Thus,

$$\begin{aligned}\Lambda_{\max}(\nabla^2 \ell(\bar{\theta}, \bar{\alpha}_{1p}; X) - \nabla^2 \ell(\theta^*, \alpha_{1p}^*; X)) &= \max_{\|u\|_2=1} u^\top \{ \nabla^2 \ell(\bar{\theta}, \bar{\alpha}_{1p}; X) - \nabla^2 \ell(\theta^*, \alpha_{1p}^*; X) \} u \\ &= \max_{\|u\|_2=1} u^\top \left\{ \frac{1}{n} \sum_{i=1}^n \left( D''(\bar{\eta}^{(i)}) - D''(\eta^*) \right) x_0^{(i)} (x_0^{(i)})^\top \right\} u.\end{aligned}$$

By Assumption 3,  $|D''(\bar{\eta}^{(i)}) - D''(\eta^*)| \leq 2\kappa_2$ , and so

$$\begin{aligned}\Lambda_{\max}(\nabla^2 \ell(\bar{\theta}, \bar{\alpha}_{1p}; X) - \nabla^2 \ell(\theta^*, \alpha_{1p}^*; X)) &= \max_{\|u\|_2=1} u^\top \left\{ \frac{1}{n} \sum_{i=1}^n (D''(\bar{\eta}^{(i)}) - D''(\eta^*)) x_0^{(i)} (x_0^{(i)})^\top \right\} u \\ &\leq 2\kappa_2 \max_{\|u\|_2=1} u^\top \left\{ \frac{1}{n} \sum_{i=1}^n x_0^{(i)} (x_0^{(i)})^\top \right\} u \leq 2\kappa_2 \Lambda_2,\end{aligned}$$

using Assumption 2 at the last inequality. Hence, we arrive at

$$\begin{aligned}
\|R^n\|_\infty &\leq \|R^n\|_2^2 = \left\| \{\nabla^2 \ell(\bar{\theta}, \bar{\alpha}_{1p}; X) - \nabla^2 \ell(\theta^*, \alpha_{1p}^*; X)\}^\top \begin{pmatrix} \hat{\theta} - \theta^* \\ \hat{\alpha}_{1p} - \alpha_{1p}^* \end{pmatrix} \right\|_2^2 \\
&\leq \Lambda_{\max}(\nabla^2 \ell(\bar{\theta}, \bar{\alpha}_{1p}; X) - \nabla^2 \ell(\theta^*, \alpha_{1p}^*; X)) \left\| \begin{pmatrix} \hat{\theta} - \theta^* \\ \hat{\alpha}_{1p} - \alpha_{1p}^* \end{pmatrix} \right\|_2^2 \\
&\leq \frac{72\kappa_2\Lambda_2}{\Lambda_1^2} (d+1)\lambda_n^2.
\end{aligned}$$

So  $\|R^n\|_\infty \leq a\lambda_n/(8-4a)$  if

$$\lambda_n \leq \frac{a}{2-a} \frac{\Lambda_1^2}{288(d+1)\kappa_2\Lambda_2}, \quad (49)$$

which holds by assumption.  $\square$

## A.7 A Proof for Corollary 1

*Proof.* The proof is essentially the same as the proof in Section A.4. We first show that a modified version of Lemma A5 holds with fewer conditions.

**Lemma 6.** *Suppose that  $p(x|x_{-s})$  follows a Gaussian distribution as in (5), and  $\|W^n\|_\infty \leq a\lambda_n/(8-4a)$ . Then*

$$\|\hat{\theta}_N - \theta_N^*\|_2 < \frac{10}{\Lambda_1} (d+1)^{1/2} \lambda_n, \quad \|R^n\|_\infty = 0.$$

*Proof.* To prove this lemma, we go through the argument in Section A.6. But for II we note that

$$\begin{aligned}
\Pi &\geq \min_{u: \|u\|_2=B, u_\Delta=0} \{-u^\top \nabla^2 \ell(\theta^* + vu_{-p}, \alpha_{1p}^* + vu_p; X)u\} \\
&\geq B^2 \Lambda_{\min}(-Q_{\Delta^c \Delta^c}^*) - \max_{v \in [0,1]} \max_{u: \|u\|_2=B, u_\Delta=0} u^\top \left( \frac{1}{n} \sum_{i=1}^n D'''(\tilde{\eta}^{(i)})(vu^\top x_0^{(i)}) x_0^{(i)} (x_0^{(i)})^\top \right) u \\
&\geq \Lambda_1 B^2 - 0,
\end{aligned}$$

since  $D'''(\tilde{\eta}^{(i)}) = 0$  for a Gaussian distribution. Therefore,

$$F(u) \geq -\frac{\lambda_n}{4} (d+1)^{1/2} B + \frac{1}{2} \Lambda_1 B^2 - \lambda_n (d+1)^{1/2} B.$$

So,  $F(u) > 0$  for  $B > 5\lambda_n(d+1)^{1/2}/(2\Lambda_1)$ . We can hence let  $B = 5(d+1)^{1/2}\lambda_n/(\Lambda_1)$  to get

$$\|\hat{\theta}_N - \theta_N^*\|_2 \leq \|\hat{u}\|_2 \leq B = \frac{5}{\Lambda_1} (d+1)^{1/2} \lambda_n.$$

Thus,  $\|\hat{\theta}_N - \theta_N^*\|_2 < 10\lambda_n(d+1)^{1/2}/\Lambda_1$ . And  $\|R^n\|_\infty = 0$  trivially as  $D''(\bar{\eta}^{(i)}) - D''(\eta^*) = 0$  for a Gaussian distribution.  $\square$

With Lemma A6, we can then verify (37) and (38) as in Section A.4. Finally, we drop the requirement of  $\xi_1$  in the condition of Lemma A6, so the probability of  $\hat{N} = N$  is

$$\text{pr} \left\{ \left( \|W^n\|_\infty \leq \frac{a}{2-a} \frac{\lambda_n}{4} \right) \cap \xi_2 \right\} \geq 1 - \exp(-c_2 \delta_2^2 n) - \exp(-c_3 \delta_3 n),$$

where  $c_2$  and  $c_3$  are constants from Proposition 3 and Lemma A4. □